



Measurement of the $W^\pm Z$ boson pair-production cross section in pp collisions at $\sqrt{s} = 13$ TeV with the ATLAS detector



The ATLAS Collaboration *

ARTICLE INFO

Article history:

Received 13 June 2016

Received in revised form 22 August 2016

Accepted 24 August 2016

Available online 6 September 2016

Editor: W.-D. Schlatter

ABSTRACT

The production of $W^\pm Z$ events in proton–proton collisions at a centre-of-mass energy of 13 TeV is measured with the ATLAS detector at the LHC. The collected data correspond to an integrated luminosity of 3.2 fb^{-1} . The $W^\pm Z$ candidates are reconstructed using leptonic decays of the gauge bosons into electrons or muons. The measured inclusive cross section in the detector fiducial region for leptonic decay modes is $\sigma_{W^\pm Z \rightarrow \ell' \nu \ell \ell}^{\text{fid.}} = 63.2 \pm 3.2 (\text{stat.}) \pm 2.6 (\text{sys.}) \pm 1.5 (\text{lumi.}) \text{ fb}$. In comparison, the next-to-leading-order Standard Model prediction is $53.4_{-2.8}^{+3.6} \text{ fb}$. The extrapolation of the measurement from the fiducial to the total phase space yields $\sigma_{W^\pm Z}^{\text{tot.}} = 50.6 \pm 2.6 (\text{stat.}) \pm 2.0 (\text{sys.}) \pm 0.9 (\text{th.}) \pm 1.2 (\text{lumi.}) \text{ pb}$, in agreement with a recent next-to-next-to-leading-order calculation of $48.2_{-1.0}^{+1.1} \text{ pb}$. The cross section as a function of jet multiplicity is also measured, together with the charge-dependent $W^+ Z$ and $W^- Z$ cross sections and their ratio.

© 2016 The Author(s). Published by Elsevier B.V. This is an open access article under the CC BY license (<http://creativecommons.org/licenses/by/4.0/>). Funded by SCOAP³.

1. Introduction

The production of $W^\pm Z$ pairs in hadron collisions is an important test of the electroweak sector of the Standard Model (SM). The $W^\pm Z$ final states arise from two vector bosons radiated by quarks or from the decay of a virtual W boson into a $W^\pm Z$ pair, which involves a triple gauge coupling (TGC). In addition, $W^\pm Z$ pairs can be produced in vector-boson scattering processes, which involve triple and quartic gauge couplings (QGC) and are sensitive to the electroweak symmetry breaking sector of the SM. New physics could manifest in $W^\pm Z$ final states as a modification of the TGC and QGC strength. Precise knowledge of the $W^\pm Z$ production cross section is therefore necessary in the search for new physics.

Measurements of the $W^\pm Z$ production cross section in proton–antiproton collisions at a centre-of-mass energy of $\sqrt{s} = 1.96$ TeV were published by the CDF and D0 Collaborations [1,2] using integrated luminosities of 7.1 fb^{-1} and 8.6 fb^{-1} , respectively. At the Large Hadron Collider (LHC), measurements have been performed in proton–proton (pp) collisions by the ATLAS Collaboration [3,4] at $\sqrt{s} = 7$ TeV and 8 TeV using integrated luminosities of 4.6 fb^{-1} and 20.3 fb^{-1} , respectively.

This Letter presents measurements of the $W^\pm Z$ production cross section in pp collisions at a centre-of-mass energy of $\sqrt{s} = 13$ TeV. The data sample analysed was collected in 2015 by the

ATLAS experiment at the LHC, and corresponds to an integrated luminosity of 3.2 fb^{-1} . The W and Z bosons are reconstructed using their decay modes into electrons or muons. The inclusive production cross section is measured in a fiducial phase space and extrapolated to the total phase space. This Letter also reports the ratio of the cross sections at 13 TeV and 8 TeV [4], as well as the ratio of the $W^+ Z/W^- Z$ cross sections, which is sensitive to the parton distribution functions (PDF). Finally, the production cross section is also measured as a function of the jet multiplicity. This distribution provides an important test of perturbative quantum chromodynamics (QCD) for diboson production processes. The $W^\pm Z$ diboson process is particularly well suited for this measurement, since the WW final state has a very large background from top-quark production when associated jets are present, and the ZZ final state has substantially fewer events. The reported measurements are compared with the SM cross-section predictions at the next-to-leading order (NLO) in QCD [5,6] and the total cross section is also compared to a very recent calculation at next-to-next-to-leading order (NNLO) in QCD [7].

2. ATLAS detector

The ATLAS detector [8] is a multi-purpose detector with a cylindrical geometry¹ and nearly 4π coverage in solid angle. The col-

* E-mail address: atlas.publications@cern.ch.

¹ ATLAS uses a right-handed coordinate system with its origin at the nominal interaction point (IP) in the centre of the detector and the z -axis along the beam

lision point is surrounded by inner tracking detectors (collectively referred to as the inner detector), followed by a superconducting solenoid providing a 2 T axial magnetic field, a calorimeter system and a muon spectrometer.

The inner detector (ID) provides precise measurements of charged-particle tracks in the pseudorapidity range $|\eta| < 2.5$. It consists of three subdetectors arranged in a coaxial geometry around the beam axis: a silicon pixel detector, a silicon microstrip detector and a transition radiation tracker. The newly installed innermost layer of pixels sensors [9,10] was operational for the first time during the 2015 data taking.

The electromagnetic calorimeter covers the region $|\eta| < 3.2$ and is based on a high-granularity, lead/liquid-argon (LAR) sampling technology. The hadronic calorimeter uses a steel/scintillator-tile detector in the region $|\eta| < 1.7$ and a copper/LAR detector in the region $1.5 < |\eta| < 3.2$. The most forward region of the detector, $3.1 < |\eta| < 4.9$, is equipped with a forward calorimeter, measuring electromagnetic and hadronic energies in copper/LAR and tungsten/LAR modules.

The muon spectrometer (MS) comprises separate trigger and high-precision tracking chambers to measure the deflection of muons in a magnetic field generated by three large superconducting toroids arranged with an eightfold azimuthal coil symmetry around the calorimeters. The high-precision chambers cover a range of $|\eta| < 2.7$. The muon trigger system covers the range $|\eta| < 2.4$ with resistive-plate chambers in the barrel and thin-gap chambers in the endcap regions.

A two-level trigger system is used to select events in real time. It consists of a hardware-based first-level trigger and a software-based high-level trigger. The latter employs algorithms similar to those used offline to identify electrons, muons, photons and jets.

3. Phase space definition

The fiducial phase space used to measure the $W^\pm Z$ cross section is defined to closely follow the criteria used to define the signal region described in Section 5. The phase space is based on the kinematics of the final-state leptons associated with the W and Z boson decays. Leptons produced in the decay of a hadron, a τ or their descendants are not considered in the definition of the fiducial phase space. In the simulation, the kinematics of the charged lepton after quantum electrodynamics (QED) final-state radiation (FSR) are “dressed” at particle level by including contributions from photons with an angular distance $\Delta R \equiv \sqrt{(\Delta\eta)^2 + (\Delta\phi)^2} < 0.1$ from the lepton. Dressed leptons, and final-state neutrinos that do not originate from hadron or τ decays, are matched to the W and Z boson decay products using a Monte Carlo generator-independent algorithmic approach, called the “resonant shape” algorithm [4], that takes into account the nominal line shapes of the W and Z resonances.

The reported cross sections are measured in a fiducial phase space defined at particle level by the following requirements: the transverse momentum p_T of the dressed leptons from the Z boson decay is above 15 GeV, the p_T of the charged lepton from the W decay is above 20 GeV, the absolute value of the pseudorapidity of the charged leptons from the W and Z bosons is below 2.5, the invariant mass of the two leptons from the Z boson decay differs at most by 10 GeV from the world average value of the Z boson mass m_Z^{PDG} [11]. The W transverse mass, defined as

$m_T^W = \sqrt{2 \cdot p_T^\nu \cdot p_T^\ell \cdot [1 - \cos \Delta\phi(\ell, \nu)]}$, where $\Delta\phi(\ell, \nu)$ is the angle between the lepton and the neutrino in the transverse plane, is required to be above 30 GeV. In addition, it is required that the angular distance ΔR between the charged leptons from the W and Z decay is larger than 0.3, and that ΔR between the two leptons from the Z decay is larger than 0.2.

The fiducial cross section is extrapolated to the total phase space and corrected for the leptonic branching fractions of the W and Z bosons. The total phase space is defined by requiring the invariant mass of the lepton pair associated with the Z boson to be in the range $66 < m_{\ell\ell} < 116$ GeV.

For the jet multiplicity differential measurement, particle-level jets are reconstructed from stable particles with a lifetime of $\tau > 30$ ps in the simulation after parton showering, hadronisation, and decay of particles with $\tau < 30$ ps. Muons, electrons, neutrinos and photons associated with W and Z decays are excluded. The particle-level jets are reconstructed with the anti- k_t algorithm [12] with a radius parameter $R = 0.4$ and are required to have a p_T above 25 GeV and an absolute value of pseudorapidity below 4.5.

4. Simulated event samples

Monte Carlo (MC) simulation is used to model signal and background processes. All generated MC events are passed through the ATLAS detector simulation [13], based on GEANT4 [14], and processed using the same reconstruction software used for the data. The event samples include the simulation of additional proton–proton interactions (pile-up) generated with PYTHIA 8.186 [15] using the MSTW2008LO PDF [16] and the A2 [17] set of tuned parameters.

Scale factors are applied to simulated events to correct for the small differences between data and MC simulation in the trigger, reconstruction, identification, isolation and impact parameter efficiencies of electrons and muons [18–20]. Furthermore, the electron energy and muon momentum in simulated events are smeared to account for small differences in resolution between data and MC [20,21].

A sample of simulated $W^\pm Z$ events is used to correct the signal yield for detector effects, to extrapolate from the fiducial to the total phase space, and to compare the measurements to the theoretical predictions. The production of $W^\pm Z$ pairs and the subsequent leptonic decays of the vector bosons are generated at NLO in QCD using the POWHEG-Box v2 [22–25] generator, interfaced to the PYTHIA 8.210 parton shower model using the AZNLO [26] set of tuned parameters. The CT10 [27] PDF set is used for the hard-scattering process, while the CTEQ6L1 [28] PDF set is used for the parton shower. The jet multiplicity measurement is also compared to the theoretical NLO prediction from the SHERPA 2.1.1 generator [29], calculated using the CT10 PDF set in conjunction with a dedicated set of tuned parameters for the parton shower developed by the SHERPA authors [30].

The background sources in this analysis include processes with two or more electroweak gauge bosons, namely ZZ , WW and VVV ($V = W, Z$); processes with top quarks, such as $t\bar{t}$ and $t\bar{t}V$, single top and tZ ; or processes with gauge bosons associated with jets or photons ($Z + j$ and $Z\gamma$). MC simulation is used to estimate the contribution from background processes with three or more prompt leptons. Background processes with at least one misidentified lepton are evaluated using data-driven techniques and simulated events are used to assess the systematic uncertainties in these backgrounds.

The $q\bar{q} \rightarrow ZZ^{(*)}$, $t\bar{t}$, and single-top processes are generated at NLO using the POWHEG-Box v2 program. The CT10 PDF set is used for the matrix-element calculations. For the ZZ process the parton shower is modelled with PYTHIA 8.186, using the

direction. The x -axis points from the IP to the centre of the LHC ring, and the y -axis points upward. Cylindrical coordinates (r, ϕ) are used in the transverse (x, y) plane, ϕ being the azimuthal angle around the beam direction. The pseudorapidity is defined in terms of the polar angle θ as $\eta = -\ln[\tan(\theta/2)]$.

CTEQ6L1 PDF and AZNLO set of tuned parameters. The modelling of the parton shower for processes with top quarks is done with PYTHIA 6.428 [31], using the CTEQ6L1 PDF and Perugia 2012 [32] set of tuned parameters. The SHERPA [29,30,33–36] event generator is used to model the $Z\gamma$, VVV , and $gg \rightarrow ZZ^{(*)}$ processes at leading order (LO) using the CT10 PDF set. Finally, the $t\bar{t}V$ and tZ processes are generated at LO using MADGRAPH5_aMC@NLO [37] with the NPDF23LO [38] PDF set, interfaced with PYTHIA 8.186 ($t\bar{t}V$) and PYTHIA 6.428 (tZ).

5. Data sample and selections

The pp collision data analysed correspond to an integrated luminosity of 3.2 fb^{-1} collected with the ATLAS detector in 2015 at $\sqrt{s} = 13 \text{ TeV}$. Only data recorded with stable beam conditions and with all relevant detector subsystems operational are considered.

Candidate events are selected using triggers [39] that require at least one electron or muon with $p_T > 24 \text{ GeV}$ or 20 GeV , respectively, that satisfies a loose isolation requirement. Possible inefficiencies for leptons with large transverse momenta are reduced by including additional electron and muon triggers that do not include any isolation requirements with transverse momentum thresholds of $p_T = 60 \text{ GeV}$ and 50 GeV , respectively. Finally, a single-electron trigger requiring $p_T > 120 \text{ GeV}$ with less restrictive electron identification criteria is used to increase the selection efficiency for high- p_T electrons.

Events are required to have a primary vertex reconstructed from at least two charged particle tracks and compatible with the luminous region. If several such vertices are present in the event, the one with the highest sum of the p_T^2 of the associated tracks is selected as the primary vertex of the $W^\pm Z$ production.

All final states with three charged leptons (electrons e or muons μ) and neutrinos from $W^\pm Z$ leptonic decays are considered. In the following, the different final states are referred to as $\mu^\pm\mu^+\mu^-$, $e^\pm\mu^+\mu^-$, $\mu^\pm e^+e^-$ and $e^\pm e^+e^-$.

Muon candidates are identified by tracks reconstructed in the muon spectrometer and matched to tracks reconstructed in the inner detector. Muons are required to pass a “medium” identification selection, which is based on requirements on the number of hits in the ID and the MS [20]. The efficiency of this selection averaged over p_T and η is larger than 98%. The muon momentum is calculated by combining the MS measurement, corrected for the energy deposited in the calorimeters, and the ID measurement. The p_T of the muon must be greater than 15 GeV and its pseudorapidity must satisfy $|\eta| < 2.5$.

Electron candidates are reconstructed from energy clusters in the electromagnetic calorimeter matched to inner detector tracks. Electrons are identified using a discriminant that is the value of a likelihood function constructed with information from the shape of the electromagnetic showers in the calorimeter, track properties and track-to-cluster matching quantities of the candidate [18]. Electrons must satisfy a “medium” likelihood requirement, which provides an overall identification efficiency of 90%. The electron momentum is computed from the cluster energy and the direction of the track. The p_T of the electron must be greater than 15 GeV and the pseudorapidity of the cluster must be in the ranges $|\eta| < 1.37$ or $1.52 < |\eta| < 2.47$.

Electron and muon candidates are required to originate from the primary vertex. Thus, the significance of the track’s transverse impact parameter calculated with respect to the beam line, $|d_0/\sigma_{d_0}|$, must be smaller than three for muons and less than five for electrons, and the longitudinal impact parameter, z_0 (the difference between the value of z of the point on the track at which d_0 is defined and the longitudinal position of the primary vertex), is required to satisfy $|z_0 \cdot \sin(\theta)| < 0.5 \text{ mm}$.

Electrons and muons are required to be isolated from other particles. The isolation requirement is based on both calorimeter and track information and is tuned for an efficiency of at least 95% for $p_T > 25 \text{ GeV}$ and at least 99% for $p_T > 60 \text{ GeV}$ [20].

Jets are reconstructed from clusters of energy deposition in the calorimeter [40] using the anti- k_t algorithm [12] with a radius parameter $R = 0.4$. Events with jets arising from detector noise or other non-collision sources are discarded [41]. All jets must have $p_T > 25 \text{ GeV}$ and be reconstructed in the pseudorapidity range $|\eta| < 4.5$. A multivariate combination of track-based variables is used to suppress jets originating from pile-up in the ID acceptance [42]. The energy of jets is calibrated and corrected for detector effects using a combination of simulated events and *in situ* methods in 13 TeV data, similar to the procedure described in Ref. [43].

The transverse momentum of the neutrino is estimated from the missing transverse momentum in the event, E_T^{miss} , calculated as the negative vector sum of the transverse momentum of all identified hard physics objects (electrons, muons, jets), as well as an additional soft term. A track-based measurement of the soft term [44], which accounts for low- p_T tracks not assigned to a hard object, is used in the analysis.

Events are required to contain exactly three lepton candidates satisfying the selection criteria described above. To ensure that the trigger efficiency is well determined, at least one of the candidate leptons is required to have $p_T > 25 \text{ GeV}$ and to be geometrically matched to a lepton that was selected by the trigger.

To suppress background processes with at least four prompt leptons, events with a fourth lepton candidate satisfying looser selection criteria are rejected. For this looser selection, the p_T of the leptons is lowered to $p_T > 7 \text{ GeV}$ and “loose” identification requirements are used for both the electrons and muons. The isolation requirement uses ID track information only and is less stringent.

Candidate events are required to have at least one pair of leptons of the same flavour and of opposite charge, with an invariant mass that is consistent with the nominal Z boson mass [11] to within 10 GeV . This pair is considered to be the Z boson candidate. If more than one pair can be formed, the pair whose invariant mass is closest to the nominal Z boson mass is taken as the Z boson candidate.

The remaining third lepton is assigned to the W boson decay. The transverse mass of the W candidate, computed using E_T^{miss} and the p_T of the associated lepton, is required to be greater than 30 GeV .

Backgrounds originating from misidentified leptons are suppressed by requiring the lepton associated with the W boson to satisfy more stringent selection criteria. Thus, the transverse momentum of these leptons is required to be greater than 20 GeV . Furthermore, electrons associated with the W boson decay are required to pass the “tight” likelihood identification requirement [18], which has an overall efficiency of 85%. Finally, these electrons must also pass a tighter isolation requirement, tuned for an efficiency of at least 90% (99%) for $p_T > 25$ (60) GeV .

6. Background estimation

The background sources are classified into two groups: events where at least one of the candidate leptons is not a prompt lepton (reducible background) and events where all candidates are prompt leptons or are produced in the decay of a τ (irreducible background). Candidates that are not prompt leptons are called also “misidentified” or “fake” leptons.

The reducible background, which represents about half of the total backgrounds, originates from $Z + j$, $Z\gamma$, $t\bar{t}$, Wt and WW

production processes, with $Z + j$ and $Z\gamma$ being the dominant component (83%). The reducible backgrounds are estimated using data-driven techniques. The background from events with two or three fake leptons, e.g., from $W + jj$ and multijet processes, is negligible.

Backgrounds from $t\bar{t}$, Wt and $WW + j$ events (called “top-like” in the following) are estimated by exploiting the different-flavour decay channels of these processes. These events are categorised based on whether the misidentified lepton is an electron or muon. The former are estimated in a control region containing $e^\pm\mu^\mp e^\pm$ events and the latter in a $\mu^\pm e^\mp\mu^\pm$ control region. Events in the control regions satisfy the selection criteria described in Section 5, except that a different-flavour, opposite-charge lepton pair is associated with the Z boson, and the $m_{\ell\ell}$ requirement is removed to increase the number of events. These requirements suppress the contamination of events with a leptonically decaying Z/γ^* . The dominant contribution is due to top-like processes (75%). The MC predictions for other processes are subtracted from the observed yield. The ratios of observed to expected top-like events in the control regions are 0.5 ± 0.3 for misidentified electrons and 1.4 ± 0.5 for misidentified muons, where the uncertainties are due to the statistical uncertainties of the data and MC events in the control regions. These ratios are applied to the estimated contributions from the simulated top-like backgrounds in the final $W^\pm Z$ selection. The kinematic shapes of the top-like background are taken from MC simulation for the purposes of control distributions and the exclusive jet multiplicity differential cross-section calculation. The shape of the jet multiplicity distribution in the top-like control regions is well modelled by the MC simulation.

Backgrounds from $Z + j$ and $Z\gamma$ processes are estimated by defining a three-lepton Z control sample in data, where two of the leptons, referred to as tight (T), meet all identification and isolation criteria described in Section 5, and the remaining lepton, referred to as loose (L), fails these requirements and instead satisfies less restrictive ones. Events in the Z control sample must satisfy all other $W^\pm Z$ selection criteria. The Z control sample is split into three categories of events, labelled as N_{LTT} , N_{TLT} and N_{TTL} , where the first index refers to the W lepton, and the second and third indexes refer to the higher- and lower- p_T leptons from the Z boson decay. The observed number of events in each of these categories is 1535, 61 and 204, respectively. The contribution from $Z + j$ and $Z\gamma$ events is greater than 75%. Processes with at least three prompt leptons are subtracted using the MC prediction. This includes the subtraction of $W^\pm Z$ events, for which the MC prediction is increased by 15% to agree with previous measurements [4]. The subtraction of top-like processes (18%) uses a procedure with a control region containing one loose lepton, analogous to the procedure described above.

The $Z + j$ and $Z\gamma$ background in the final $W^\pm Z$ selection is obtained by scaling the observed number of events in the Z control sample by an extrapolation factor called the “fake factor”. The fake factor is measured in a data sample with two tight leptons associated with the Z boson and one additional lepton that can be loose or tight. To enrich the sample in $Z + j$ and $Z\gamma$ events, the m_T^W requirement is reversed and the missing transverse momentum is required to be less than 40 GeV. The fake factor is calculated as the ratio of the number of events with a tight third lepton to the number of events with a loose third lepton. The dominant contribution (>97%) to the denominator of the fake-factor ratio originates from $Z + j$ and $Z\gamma$ events. Simulation shows that the relative fractions of these two processes are similar in this region and the Z control sample where the fake factor is applied, justifying the use of a single fake factor to describe both backgrounds. Processes with at least three prompt leptons contaminate the events in the numerator of the ratio, particularly at high lepton p_T , and are subtracted

as described for the Z control sample. The fake factor is computed in bins of p_T of the lepton not associated with the Z boson, separately for muons and electrons, and considering the different selection criteria used for leptons in the analysis. MC simulation is used to verify that the fake factors do not depend on the jet multiplicity of the event. The fake-factor values range between 0.02 and 0.1.

In brief, the $Z + j$ and $Z\gamma$ estimate in each lepton p_T bin is obtained by extrapolating from events in the Z control sample using the following formula:

$$N_{Z+j/Z\gamma} = \left(N_{LTT} - N_{LTT}^{\text{prompt}} - N_{LTT}^{\text{top}} \right) F_W \\ + \left(N_{TLT} - N_{TLT}^{\text{prompt}} - N_{TLT}^{\text{top}} \right) F_Z \\ + \left(N_{TTL} - N_{TTL}^{\text{prompt}} - N_{TTL}^{\text{top}} \right) F_Z, \quad (1)$$

where F_W and F_Z denote the fake factors for W and Z leptons, N_{LTT}^{prompt} , N_{TLT}^{prompt} and N_{TTL}^{prompt} denote the MC prediction of processes with at least three prompt leptons, and N_{LTT}^{top} , N_{TLT}^{top} and N_{TTL}^{top} denote the estimate of top-like events. Both the normalisation and the kinematic shapes of the $Z + j$ and $Z\gamma$ background are estimated from the data using this methodology. The estimate of the $Z + j$ and $Z\gamma$ background is validated in a subset of the signal region containing events with $30 < m_T^W < 50$ GeV and $E_T^{\text{miss}} < 40$ GeV, which is enriched in background processes.

The reducible background was also assessed with an alternative procedure, the matrix method, used in the previous measurement of $W^\pm Z$ production at $\sqrt{s} = 8$ TeV from the ATLAS Collaboration [4]. The results agree with the estimates described above within 5%.

Irreducible background events originate from ZZ , $t\bar{t} + V$, VVV (where $V = Z$ or W), tZ and $W^\pm Z$ events in which at least one of the bosons decays into leptons via an intermediate τ decay. The amount of irreducible background is estimated using MC simulations. The estimate of the contribution from $W^\pm Z$ events decaying via τ -leptons is addressed in Section 8.

About 70% of the irreducible background is due to ZZ production. Events from ZZ production survive the $W^\pm Z$ event selection either because one lepton falls outside the fiducial volume or because it falls in the fiducial acceptance of the detector but is not identified. The number of $q\bar{q} \rightarrow ZZ$ events predicted by POWHEG is scaled by 1.08 to account for NNLO QCD and NLO EW corrections [45–47]. The number of $gg \rightarrow ZZ$ events predicted by the SHERPA MC event sample is scaled by a factor of 1.52 to account for NLO QCD corrections [48]. These estimates are validated by comparing the MC predictions with the observed event yield, and the distributions of several kinematic variables, in a four-lepton data sample enriched in ZZ events. The number of observed events in this validation region is 106, with 89% purity for the ZZ process. Overall agreement between the data and the predictions is within one standard deviation of the experimental uncertainty. The shapes of the distributions of the main kinematic variables are also found to be well described by the MC predictions.

7. Detector-level results

Table 1 summarises the predicted and observed numbers of events together with the estimated background contributions. The total uncertainties affecting the predicted yields include statistical uncertainties, the theoretical uncertainties in the cross sections as further discussed in Section 10, experimental uncertainties discussed in Section 9 and uncertainty in the integrated luminosity for backgrounds estimated using MC predictions. Fig. 1 shows the

Table 1

Observed and expected numbers of events after the $W^\pm Z$ inclusive selection described in Section 5 in each of the considered channels and for the sum of all channels. The expected number of $W^\pm Z$ events from POWHEG+PYTHIA and the estimated number of background events from other processes are detailed. The total uncertainties quoted include the statistical uncertainties, the theoretical uncertainties in the cross sections, the experimental uncertainties and the uncertainty in the integrated luminosity.

Channel	eee	μee	$e\mu\mu$	$\mu\mu\mu$	All
Data	98	122	166	183	569
Total expected	102 ± 10	118 ± 9	126 ± 11	160 ± 12	506 ± 38
WZ	74 ± 6	96 ± 8	97 ± 8	129 ± 10	396 ± 32
$Z + j, Z\gamma$	16 ± 7	7 ± 5	14 ± 7	9 ± 5	45 ± 17
ZZ	6.7 ± 0.7	8.7 ± 1.0	8.5 ± 0.9	11.7 ± 1.2	36 ± 4
$t\bar{t} + V$	2.7 ± 0.4	3.2 ± 0.4	2.9 ± 0.4	3.4 ± 0.5	12.1 ± 1.6
$t\bar{t}, Wt, WW + j$	1.2 ± 0.8	2.0 ± 0.9	2.4 ± 0.9	3.6 ± 1.5	9.2 ± 3.1
tZ	1.28 ± 0.20	1.65 ± 0.26	1.63 ± 0.26	2.12 ± 0.34	6.7 ± 1.1
VVV	0.24 ± 0.04	0.29 ± 0.05	0.27 ± 0.04	0.34 ± 0.05	1.14 ± 0.18

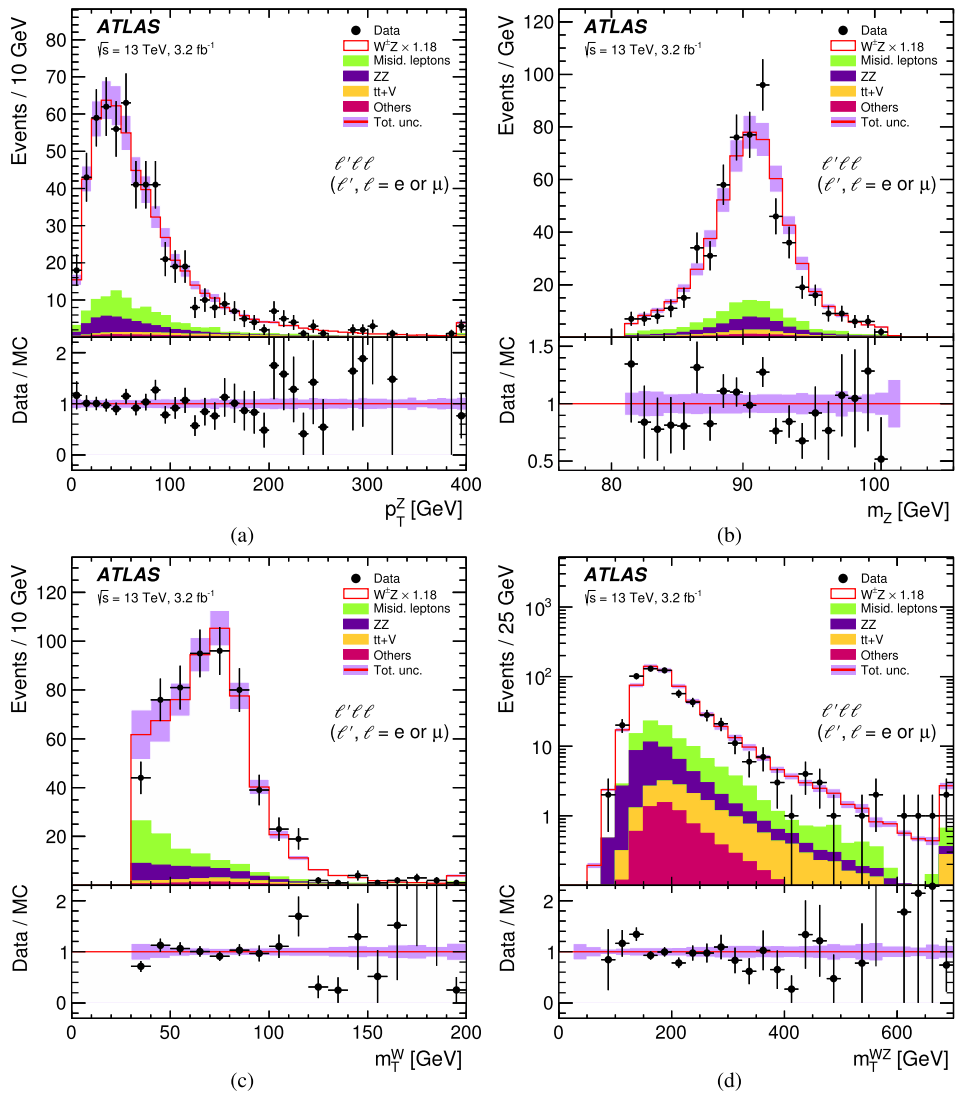


Fig. 1. The distributions for the sum of all channels of the kinematic variables (a) the transverse momentum of the reconstructed Z boson p_T^Z , (b) the reconstructed Z boson mass m_Z , (c) the transverse mass of the reconstructed W boson m_T^W and (d) the transverse mass variable m_T^{WZ} for the WZ system. The points correspond to the data, and the histograms correspond to the predictions of the different SM processes. All Monte Carlo predictions are scaled to the integrated luminosity of the data using the predicted MC cross sections of each sample. The sum of the background processes with misidentified leptons is labelled “Misid. leptons”. The POWHEG+PYTHIA MC prediction is used for the $W^\pm Z$ signal contribution. It is scaled by a global factor of 1.18 to match the measured inclusive $W^\pm Z$ cross section. The open red histogram shows the total prediction; the shaded violet band is the total uncertainty of this prediction. The last bin contains the overflow. The lower panels in each figure show the ratio of the data points to the open red histogram with their respective uncertainties. (For interpretation of the references to colour in this figure legend, the reader is referred to the web version of this article.)

Table 2

The C_{WZ} and N_τ/N_{all} factors for each of the eee , μee , $e\mu\mu$, and $\mu\mu\mu$ inclusive channels. The POWHEG+PYTHIA MC event sample with the “resonant shape” lepton assignment algorithm at particle level is used. Only statistical uncertainties are reported.

Channel	C_{W-Z}	C_{W+Z}	$C_{W^\pm Z}$	N_τ/N_{all}
eee	0.428 ± 0.005	0.417 ± 0.004	0.421 ± 0.003	0.040 ± 0.001
μee	0.556 ± 0.006	0.550 ± 0.005	0.553 ± 0.004	0.038 ± 0.001
$e\mu\mu$	0.550 ± 0.006	0.553 ± 0.005	0.552 ± 0.004	0.036 ± 0.001
$\mu\mu\mu$	0.729 ± 0.007	0.734 ± 0.006	0.732 ± 0.005	0.040 ± 0.001

measured distributions of the transverse momentum and the invariant mass of the Z candidate, the transverse mass of the W candidate, and for the WZ system a variable m_T^{WZ} [4] similar to the transverse mass. The POWHEG+PYTHIA MC prediction is used for the $W^\pm Z$ signal contribution. In Fig. 1 this contribution is scaled by a global factor of 1.18 to match the measured inclusive $W^\pm Z$ cross section in Section 10. This scaling is only used for an illustrative purpose in this figure and does not affect the measurements. Fig. 1 indicates that the MC predictions provide a fair description of the shapes of the data distributions.

8. Corrections for detector effects and acceptance

For a given channel $W^\pm Z \rightarrow \ell'^\pm \nu \ell^+ \ell^-$, where ℓ and ℓ' are either an electron or a muon, the integrated fiducial cross section, which includes the leptonic branching fractions of the W and Z , is calculated as

$$\sigma_{W^\pm Z \rightarrow \ell' \nu \ell \ell}^{\text{fid.}} = \frac{N_{\text{data}} - N_{\text{bkg}}}{\mathcal{L} \cdot C_{WZ}} \times \left(1 - \frac{N_\tau}{N_{\text{all}}}\right), \quad (2)$$

where N_{data} is the number of observed events, N_{bkg} is the estimated number of background events, \mathcal{L} is the integrated luminosity and C_{WZ} , obtained from simulation, is the ratio of the number of selected signal events at detector level to the number of events at particle level in the fiducial phase space defined after QED FSR. This factor corrects for detector efficiency and resolution effects and for QED FSR effects. The term in parentheses represents the correction applied to the measurement to account for the τ -lepton contribution to the analysis phase space. This contribution is estimated using the simulation, from the ratio of N_τ , the number of selected events in which at least one of the bosons decays into a τ lepton, and N_{all} , the number of selected WZ events with decays into any lepton.

The C_{WZ} factors for the W^-Z , W^+Z and $W^\pm Z$ inclusive processes, as well as the τ -lepton contribution to the analysis phase space, N_τ/N_{all} , are computed with POWHEG+PYTHIA for each of the four leptonic channels and are shown in Table 2.

The total cross section is calculated as

$$\sigma_{W^\pm Z}^{\text{tot.}} = \frac{\sigma_{W^\pm Z \rightarrow \ell' \nu \ell \ell}^{\text{fid.}}}{\mathcal{B}_W \mathcal{B}_Z A_{WZ}}, \quad (3)$$

where $\mathcal{B}_W = 10.86 \pm 0.09\%$ and $\mathcal{B}_Z = 3.3658 \pm 0.0023\%$ are the W and Z leptonic branching fractions [11], respectively, and A_{WZ} is the acceptance factor calculated at particle level as the ratio of the number of events in the fiducial phase space to the number of events in the total phase space as defined in Section 3.

A single acceptance factor of $A_{WZ} = 0.343 \pm 0.002$ (stat.) is obtained using the POWHEG+PYTHIA simulation by averaging the acceptance factors computed in the μee and $e\mu\mu$ channels. The use of these channels avoids the ambiguity arising from the assignment at particle level of final-state leptons to the W and Z bosons. Cross-section differences between $\ell'\ell\ell$ and $\ell\ell\ell$ channels caused by interference effects due to the three identical leptons in the $\ell\ell\ell$ final states are shown by simulation to be below 1%.

The differential detector-level distribution of the exclusive jet multiplicity is corrected for detector resolution and for QED FSR effects using an iterative Bayesian unfolding method [49,50]. Simulated signal events from POWHEG+PYTHIA are used to obtain a response matrix that accounts for bin-to-bin migration effects between the reconstructed and particle-level distribution.

9. Systematic uncertainties

The systematic uncertainties in the measured cross sections are due to experimental and theoretical uncertainties in the acceptance, uncertainties in the correction procedure for detector effects, uncertainties in the background estimation and uncertainties in the luminosity.

The theoretical systematic uncertainties in the A_{WZ} and C_{WZ} factors are evaluated by taking into account the uncertainties related to the choice of PDF set, to the QCD renormalisation μ_R and factorisation μ_F scales and to the parton showering simulation. The uncertainties due to the choice of PDF are computed using the CT10 eigenvectors and the envelope of the differences between the CT10 and CT14 [51], MMHT2014 [52] and NNPDF 3.0 [53] PDF sets, according to the PDF4LHC recommendations [54]. The QCD scale uncertainties are estimated by varying μ_R and μ_F by factors of two around the nominal scale $m_{WZ}/2$ with the constraint $0.5 \leq \mu_R/\mu_F \leq 2$, where m_{WZ} is the invariant mass of the WZ system. Uncertainties arising from the choice of parton shower model are obtained from Ref. [4]. None of the three sources of theoretical uncertainty have a significant effect on the C_{WZ} factors. The uncertainty in the acceptance factor A_{WZ} is less than 0.5% due to PDF choice, and less than 0.7% due to QCD scale choice.

The uncertainty in the unfolded jet multiplicity distribution arising from the MC modelling of the response matrix in the unfolding procedure is estimated by reweighting the simulated events at particle level to match the unfolded results obtained as described in Section 8. An alternative response matrix is defined using these reweighted MC events and is used to unfold the POWHEG+PYTHIA reconstructed events. The systematic uncertainty is estimated by comparing this unfolded distribution to the original particle-level POWHEG+PYTHIA prediction. The size of this uncertainty is at most 15%.

The experimental systematic uncertainty in the C_{WZ} factors and in the unfolding procedure includes uncertainties in the scale and resolution of the electron energy, muon momentum, jet energy and E_T^{miss} , as well as uncertainties in the scale factors applied to the simulation in order to reproduce the trigger, reconstruction, identification and isolation efficiencies measured in data. The uncertainties in the jet energy scale are obtained from $\sqrt{s} = 13$ TeV simulations and *in situ* measurements, similar to the ones described in Ref. [43]. The uncertainty in the jet energy resolution is derived by extrapolating measurements in Run-1 data to $\sqrt{s} = 13$ TeV. The uncertainty in the E_T^{miss} is estimated by propagating the uncertainties in the transverse momenta of hard physics objects and by applying momentum scale and resolution uncertainties to the track-based soft term. The uncertainty associated with pile-up modelling is of the order of 1% and can reach up to 2.9% in the 0-jet bin of the unfolded jet multiplicity distribution. For the measurements of the W charge-dependent cross sections, an uncertainty arising from the charge misidentification of leptons is also considered. It affects only electrons and leads to an uncertainty of less than 0.05% in the ratio of W^+Z to W^-Z integrated cross sections determined by combining the four decay channels.

The dominant contribution among the experimental systematic uncertainties in the eee and μee channels is due to the uncertainty in the electron identification efficiency, contributing at most 1.4% uncertainty to the integrated cross section, while in the $e\mu\mu$

and $\mu\mu\mu$ channels it originates from the muon reconstruction efficiency and is at most 1.1%. The systematic uncertainties in the measured cross sections are determined by repeating the analysis after applying appropriate variations for each source of systematic uncertainty to the simulated samples.

The dominant uncertainty in the reducible $t\bar{t}$, Wt and $WW + j$ background arises from the number of data and MC events in the control regions used to estimate the top-like processes and amounts to 32% of the estimated yield. An uncertainty of 2% is assigned due to the extrapolation from the control regions to the $W^\pm Z$ signal region.

The statistical precision of 3% in the reducible $Z + j$ and $Z\gamma$ background estimate is determined by the size of the N_{LTT} , N_{TLT} and N_{TTL} categories in the Z control sample. Uncertainties due to the size of the sample used to derive the fake factor amount to 21% of the estimated $Z + j$ and $Z\gamma$ yield. An uncertainty of 15% is assigned to the contributions from processes with at least three prompt leptons, which are subtracted from the sample used to derive the fake factor. This has an 18% impact on the $Z + j$ and $Z\gamma$ estimate. The uncertainty due to the subtraction of $t\bar{t}$, Wt and WW processes is smaller than 2%. To account for differences between the region in which the fake factor is calculated and the Z control sample where it is applied, including the different relative contributions from $Z + j$ and $Z\gamma$ processes in each region, the fake factor is calculated using MC events in both regions, and the full difference between the two is taken as a systematic uncertainty, representing 26% of the estimated $Z + j$ and $Z\gamma$ yield. Overall, the $Z + j$ and $Z\gamma$ background is estimated with a precision of 38%.

A theoretical uncertainty in the ZZ cross section of 8% [45–48] is assigned as a global uncertainty in the amount of ZZ background predicted by the MC simulation. An additional uncertainty of 3% to 6% is assigned due to the correction applied to ZZ MC events with unidentified leptons.

The uncertainty due to other irreducible background sources is evaluated by propagating the uncertainty in their MC cross sections. These are 13% (12%) for $t\bar{t}W$ ($t\bar{t}Z$) [37], 20% for VVV [55] and 15% for tZ [4].

An uncertainty in the integrated luminosity of 2.1% is applied to the signal normalisation as well as to all background contributions that are estimated purely using MC simulations. The uncertainty is derived following a methodology similar to that detailed in Refs. [56,57], from a calibration of the luminosity scale using x - y beam-separation scans performed in August 2015. It has an effect of 2.4% on the measured cross sections.

The total systematic uncertainty in the $W^\pm Z$ fiducial cross section, excluding the luminosity uncertainty, varies between 4% and 10% for the four different measurement channels, and is dominated by the uncertainty in the reducible background estimate. The statistical uncertainty in the fiducial cross-section measurement is slightly larger than the systematic uncertainty. Table 3 shows the statistical uncertainty and main sources of systematic uncertainty in the $W^\pm Z$ fiducial cross section for each of the four channels and their combination.

10. Cross-section measurements

The measured fiducial cross sections in the four channels are combined using a χ^2 minimisation method that accounts for correlations between the sources of systematic uncertainty affecting each channel [58–60]. The combination of the $W^\pm Z$ cross sections in the fiducial phase space yields a total χ^2 per degree of freedom (n_{dof}) of $\chi^2/n_{\text{dof}} = 6.9/3$. The combinations of the W^+Z and the W^-Z cross sections separately yield $\chi^2/n_{\text{dof}} = 5.3/3$ and $2.0/3$, respectively.

Table 3

Summary of the relative uncertainties in the measured fiducial cross section $\sigma_{W^\pm Z}^{\text{fid}}$ for each channel and for their combination. The uncertainties are reported as percentages. The decomposition of the total systematic uncertainty into the main sources correlated between channels and the source uncorrelated between channels is indicated in the first rows.

	eee	μee	$e\mu\mu$	$\mu\mu\mu$	Combined
Relative uncertainties [%]					
e energy scale	0.5	0.2	0.3	<0.1	0.2
e id. efficiency	1.4	1.1	0.6	—	0.7
μ momentum scale	<0.1	<0.1	<0.1	0.1	<0.1
μ id. efficiency	—	0.6	1.0	1.4	0.7
$E_{\text{T}}^{\text{miss}}$ and jets	0.3	0.4	0.8	0.7	0.6
Trigger	<0.1	0.1	0.1	0.2	0.1
Pile-up	0.7	1.1	1.0	0.7	0.9
Misid. lepton background	10	4.6	4.8	3.2	3.6
ZZ background	1.0	0.7	0.6	0.7	0.7
Other backgrounds	0.5	0.5	0.3	0.3	0.4
Uncorrelated	2.2	1.3	1.4	1.7	0.8
Total sys. uncertainty	11	5.1	5.3	4.1	4.1
Luminosity	2.4	2.4	2.3	2.3	2.4
Statistics	14	11	10	8.8	5.1
Total	18	12	11	10	7.0

Combining the four channels to obtain a weighted mean value, the cross section of $W^\pm Z$ production and decay to a single leptonic channel with muons or electrons in the detector fiducial region is

$$\sigma_{W^\pm Z \rightarrow \ell' \nu \ell \ell}^{\text{fid}} = 63.2 \pm 3.2 (\text{stat.}) \pm 2.6 (\text{sys.}) \pm 1.5 (\text{lumi.}) \text{ fb.} \quad (4)$$

The SM NLO QCD prediction from POWHEG+PYTHIA is $53.4^{+1.6}_{-1.2} (\text{PDF})^{+2.1}_{-1.6} (\text{scale}) \text{ fb}$. The theoretical predictions are estimated using the CT10 PDF set and setting the dynamic QCD scales, μ_R and μ_F , equal to $m_{WZ}/2$. The uncertainty in the theoretical prediction due to the PDF is estimated using the eigenvectors of the CT10 PDF set scaled to 68% confidence level (CL) and the envelope of the differences between the results obtained with the CT14 [51], MMHT2014 [52] and NNPDF3.0 [53] NLO PDF sets. The QCD scale uncertainty is estimated conventionally by varying the scales μ_R and μ_F by factors of two around the nominal value of $m_{WZ}/2$ with the constraint $0.5 \leq \mu_R/\mu_F \leq 2$. The measured $W^\pm Z$ production cross sections are compared to the SM NLO prediction from POWHEG+PYTHIA in Fig. 2 and all results for $W^\pm Z$, W^+Z and W^-Z final states are reported in Table 4. The measured cross section is larger than the SM prediction, as also were the corresponding cross-section measurements performed at lower centre-of-mass energies by the ATLAS Collaboration [3,4].

Using the integrated fiducial cross section measured for $W^\pm Z$ production at $\sqrt{s} = 8 \text{ TeV}$ from Ref. [4], the ratio $\sigma_{W^\pm Z}^{\text{fid}, 13 \text{ TeV}} / \sigma_{W^\pm Z}^{\text{fid}, 8 \text{ TeV}}$ of the $W^\pm Z$ production cross sections at the two centre-of-mass energies of 8 and 13 TeV is calculated and yields

$$\frac{\sigma_{W^\pm Z}^{\text{fid}, 13 \text{ TeV}}}{\sigma_{W^\pm Z}^{\text{fid}, 8 \text{ TeV}}} = 1.80 \pm 0.10 (\text{stat.}) \pm 0.08 (\text{sys.}) \pm 0.06 (\text{lumi.}). \quad (5)$$

All uncertainties are treated as uncorrelated between the measurements at the two beam energies. The measured ratio is in good agreement with the Standard Model prediction of 1.78 ± 0.03 from POWHEG+PYTHIA.

The ratio of W^+Z to W^-Z production cross sections is

$$\frac{\sigma_{W^+Z \rightarrow \ell' \nu \ell \ell}^{\text{fid}}}{\sigma_{W^-Z \rightarrow \ell' \nu \ell \ell}^{\text{fid}}} = 1.39 \pm 0.14 (\text{stat.}) \pm 0.03 (\text{sys.}). \quad (6)$$

Most of the systematic uncertainties, and especially the luminosity uncertainty, cancel in the ratio, and the measurement

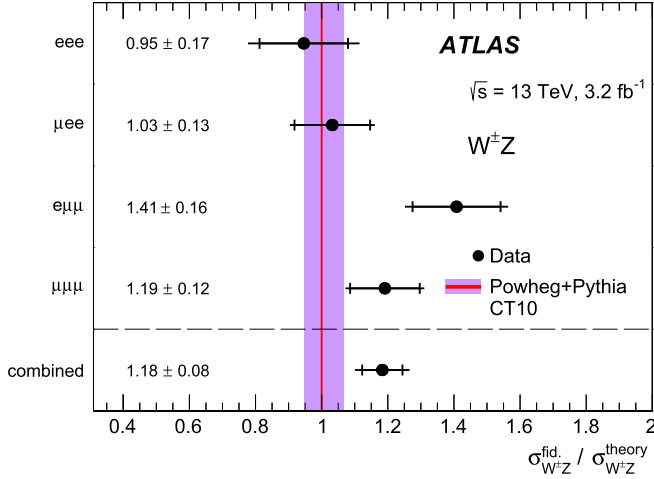


Fig. 2. Ratio of the measured $W^\pm Z$ integrated cross sections in the fiducial phase space to the NLO SM prediction from POWHEG+PYTHIA in each of the four channels and for their combination. The inner and outer error bars on the data points represent the statistical and total uncertainties, respectively. The NLO SM prediction from POWHEG+PYTHIA using the CT10 PDF set is represented by the red line; the shaded violet band is the total uncertainty in this prediction. (For interpretation of the references to colour in this figure legend, the reader is referred to the web version of this article.)

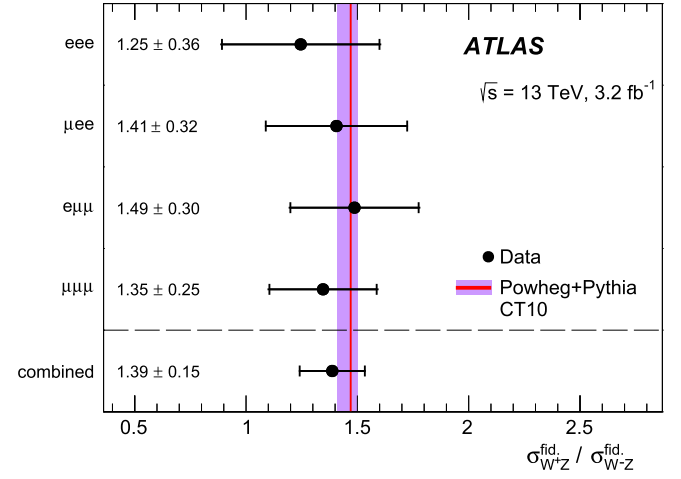


Fig. 3. Measured ratios $\sigma_{W^\pm Z}^{\text{fid.}} / \sigma_{W^\pm Z}^{\text{fid.}}$ of $W^\pm Z$ and $W^- Z$ integrated cross sections in the fiducial phase space in each of the four channels and for their combination. The error bars on the data points represent the total uncertainties, which are dominated by the statistical uncertainties. The NLO SM prediction from POWHEG+PYTHIA using the CT10 PDF set is represented by the red line; the shaded violet band is the total uncertainty in this prediction. (For interpretation of the references to colour in this figure legend, the reader is referred to the web version of this article.)

Table 4

Fiducial integrated cross section in fb, for $W^\pm Z$, $W^+ Z$ and $W^- Z$ production, measured in each of the eee , μee , $e\mu\mu$, and $\mu\mu\mu$ channels and all four channels combined. The statistical ($\delta_{\text{stat.}}$), total systematic ($\delta_{\text{sys.}}$), luminosity ($\delta_{\text{lumi.}}$) and total ($\delta_{\text{tot.}}$) uncertainties are given in percent.

Channel	$\sigma^{\text{fid.}}$ [fb]	$\delta_{\text{stat.}}$ [%]	$\delta_{\text{sys.}}$ [%]	$\delta_{\text{lumi.}}$ [%]	$\delta_{\text{tot.}}$ [%]
$\sigma_{W^\pm Z \rightarrow \ell' \nu \ell \ell}^{\text{fid.}}$					
$e^\pm ee$	50.5	14.2	10.6	2.4	17.8
$\mu^\pm ee$	55.1	11.1	5.1	2.4	12.4
$e^\pm \mu\mu$	75.2	9.5	5.3	2.3	11.1
$\mu^\pm \mu\mu$	63.6	8.9	4.1	2.3	10.0
Combined	63.2	5.2	4.1	2.4	7.0
SM prediction	53.4	—	—	—	6.0
$\sigma_{W^+ Z \rightarrow \ell' \nu \ell \ell}^{\text{fid.}}$					
$e^+ ee$	28.0	19.2	11.2	2.4	22.3
$\mu^+ ee$	32.2	14.4	5.0	2.4	15.3
$e^+ \mu\mu$	45.0	12.1	4.6	2.3	13.1
$\mu^+ \mu\mu$	36.5	11.6	4.1	2.3	12.5
Combined	36.7	6.7	3.9	2.3	8.1
SM prediction	31.8	—	—	—	5.8
$\sigma_{W^- Z \rightarrow \ell' \nu \ell \ell}^{\text{fid.}}$					
$e^- ee$	22.5	21.0	10.5	2.4	23.6
$\mu^- ee$	22.9	17.5	5.8	2.4	18.5
$e^- \mu\mu$	30.2	15.2	6.9	2.3	16.8
$\mu^- \mu\mu$	27.1	13.7	5.0	2.4	14.7
Combined	26.1	8.1	4.7	2.4	9.6
SM prediction	21.6	—	—	—	7.9

is dominated by the statistical uncertainty. The measured cross-section ratios, for each channel and for their combination, are compared in Fig. 3 to the SM prediction of $1.47^{+0.03}_{-0.06}$, which is calculated with POWHEG+PYTHIA and the CT10 PDF set.

The combined fiducial cross section is extrapolated to the total phase space. The result is

$$\sigma_{W^\pm Z}^{\text{tot.}} = 50.6 \pm 2.6(\text{stat.}) \pm 2.0(\text{sys.}) \pm 0.9(\text{th.}) \pm 1.2(\text{lumi.}) \text{ pb}, \quad (7)$$

where the theoretical uncertainty accounts for the uncertainties in the A_{WZ} factor due to the choice of PDF set, QCD scales and parton shower model. The NLO SM prediction calculated with POWHEG+PYTHIA is $42.4 \pm 0.8(\text{PDF}) \pm 1.6(\text{scale})$ pb. A recent calculation [7] of the $W^\pm Z$ production cross section at NNLO in QCD with MATRIX, obtained using the NNPDF3.0 PDF set and with μ_R and μ_F scales fixed to $(m_W + m_Z)/2$, yields $48.2^{+1.1}_{-1.0}(\text{scale})$ pb, which is in better agreement with the measurement. As this prediction does not include effects of QED final-state radiation, a correction factor of 0.972 as estimated from POWHEG+PYTHIA is applied.

Finally, the exclusive jet multiplicity cross section is presented in Fig. 4 and compared to the predictions from POWHEG+PYTHIA and SHERPA. The shape of the measured cross section as a function of jet multiplicity is described well by SHERPA, but it is reproduced poorly by POWHEG+PYTHIA. The matrix-element calculation in the SHERPA prediction includes up to three jets at LO, while in the POWHEG+PYTHIA prediction only the leading jet is included, and higher jet multiplicities are described by the parton shower models.

11. Conclusion

Measurements of $W^\pm Z$ production in $\sqrt{s} = 13$ TeV pp collisions at the LHC are presented. The data were collected with the ATLAS detector in 2015 and correspond to an integrated luminosity of 3.2 fb^{-1} . The measurements use leptonic decay modes of the gauge bosons to electrons or muons and are performed in a fiducial phase space closely matching the detector acceptance. The measured inclusive cross section in the fiducial region for one leptonic decay channel is $\sigma_{W^\pm Z \rightarrow \ell' \nu \ell \ell}^{\text{fid.}} = 63.2 \pm 3.2(\text{stat.}) \pm 2.6(\text{sys.}) \pm 1.5(\text{lumi.}) \text{ fb}$. The NLO Standard Model prediction from POWHEG+PYTHIA is $53.4^{+3.6}_{-2.8} \text{ fb}$. The measured cross section is higher than the SM NLO prediction; a similar excess was found in the cross-section measurements performed at lower centre-of-mass energies by the ATLAS Collaboration.

The ratio of the measured cross sections at the two centre-of-mass energies yields $\sigma_{W^\pm Z}^{\text{fid.}, 13 \text{ TeV}} / \sigma_{W^\pm Z}^{\text{fid.}, 8 \text{ TeV}} = 1.80 \pm 0.10(\text{stat.}) \pm 0.08(\text{sys.}) \pm 0.06(\text{lumi.})$, in good agreement with the SM NLO prediction of 1.78 ± 0.03 from POWHEG+PYTHIA. The $W^+ Z$ and

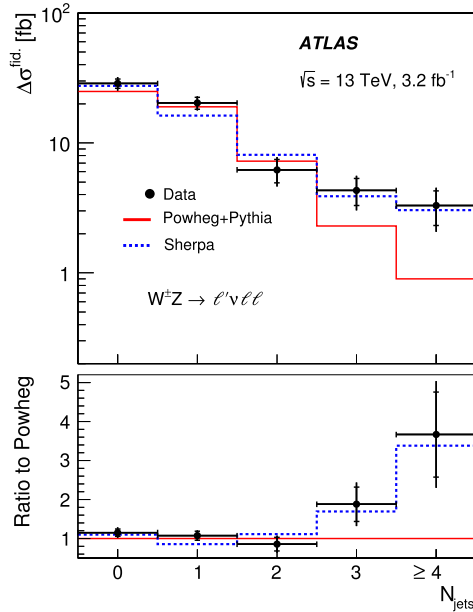


Fig. 4. The measured $W^{\pm}Z$ differential cross section in the fiducial phase space as a function of the exclusive jet multiplicity of jets with $p_{T} > 25$ GeV. The inner and outer error bars on the data points represent the statistical and total uncertainties, respectively. The measurements are compared to the prediction from POWHEG+PYTHIA (red line) and SHERPA (dashed blue line). (For interpretation of the references to colour in this figure legend, the reader is referred to the web version of this article.)

$W^{\pm}Z$ production cross sections are measured separately in the fiducial phase space and are reported; their ratio is $\sigma_{W^{\pm}Z \rightarrow \ell'\nu\ell\ell}^{\text{fid}} / \sigma_{W^{\pm}Z \rightarrow \ell'\nu\ell\ell}^{\text{fid}} = 1.39 \pm 0.14(\text{stat.}) \pm 0.03(\text{sys.})$. This result is in agreement with the SM NLO expectation from POWHEG+PYTHIA of $1.47^{+0.03}_{-0.06}$. The measured cross section extrapolated to the total phase space is $50.6 \pm 2.6(\text{stat.}) \pm 2.0(\text{sys.}) \pm 0.9(\text{th.}) \pm 1.2(\text{lumi.})$ pb, in very good agreement with the SM NNLO prediction from MATRIX of $48.2^{+1.1}_{-1.0}$ (scale) pb.

Finally, the $W^{\pm}Z$ production cross section is measured as a function of the exclusive jet multiplicity and compared to the SM predictions of POWHEG+PYTHIA and SHERPA. The SHERPA prediction is found to provide a better description of the data, at low and high jet multiplicities.

Acknowledgements

We thank CERN for the very successful operation of the LHC, as well as the support staff from our institutions without whom ATLAS could not be operated efficiently.

We acknowledge the support of ANPCyT, Argentina; YerPhI, Armenia; ARC, Australia; BMWFW and FWF, Austria; ANAS, Azerbaijan; SSTC, Belarus; CNPq and FAPESP, Brazil; NSERC, NRC and CFI, Canada; CERN; CONICYT, Chile; CAS, MOST and NSFC, China; COLCIENCIAS, Colombia; MSMT CR, MPO CR and VSC CR, Czech Republic; DNRF and DNSRC, Denmark; IN2P3-CNRS, CEA-DSM/IRFU, France; GNSF, Georgia; BMBF, HGF, and MPG, Germany; GSRT, Greece; RGC, Hong Kong SAR, China; ISF, I-CORE and Benoziyo Center, Israel; INFN, Italy; MEXT and JSPS, Japan; CNRST, Morocco; FOM and NWO, Netherlands; RCN, Norway; MNiSW and NCN, Poland; FCT, Portugal; MNE/IFA, Romania; MES of Russia and NRC KI, Russian Federation; JINR; MESTD, Serbia; MSSR, Slovakia; ARRS and MIZŠ, Slovenia; DST/NRF, South Africa; MINECO, Spain; SRC and Knut and Alice Wallenberg Foundation, Sweden; SERI, SNSF and Cantons of Bern and Geneva, Switzerland; MOST, Taiwan; TAEK, Turkey; STFC, United Kingdom; DOE and NSF, United

States of America. In addition, individual groups and members have received support from BCKDF, the Canada Council, Canarie, CRC, Compute Canada, FQRNT, and the Ontario Innovation Trust, Canada; EPLANET, ERC, FP7, Horizon 2020 and Marie Skłodowska-Curie Actions, European Union; Investissements d'Avenir Labex and Idex, ANR, Région Auvergne and Fondation Partager le Savoir, France; DFG and AvH Foundation, Germany; Herakleitos, Thales and Aristeia programmes co-financed by EU-ESF and the Greek NSRF; BSF, GIF and Minerva, Israel; BRF, Norway; Generalitat de Catalunya, Generalitat Valenciana, Spain; the Royal Society and Leverhulme Trust, United Kingdom.

The crucial computing support from all WLCG partners is acknowledged gratefully, in particular from CERN, the ATLAS Tier-1 facilities at TRIUMF (Canada), NDGF (Denmark, Norway, Sweden), CC-IN2P3 (France), KIT/GridKA (Germany), INFN-CNAF (Italy), NL-T1 (Netherlands), PIC (Spain), ASGC (Taiwan), RAL (UK) and BNL (USA), the Tier-2 facilities worldwide and large non-WLCG resource providers. Major contributors of computing resources are listed in Ref. [61].

References

- [1] CDF Collaboration, T. Aaltonen, et al., Measurement of the WZ cross section and triple gauge couplings in pp collisions at $\sqrt{s} = 1.96$ TeV, *Phys. Rev. D* 86 (2012) 031104, arXiv:1202.6629 [hep-ex].
- [2] D0 Collaboration, V.M. Abazov, et al., A measurement of the WZ and ZZ production cross sections using leptonic final states in 8.6 fb^{-1} of pp collisions, *Phys. Rev. D* 85 (2012) 112005, arXiv:1201.5652 [hep-ex].
- [3] ATLAS Collaboration, Measurement of WZ production in proton–proton collisions at $\sqrt{s} = 7$ TeV with the ATLAS detector, *Eur. Phys. J. C* 72 (2012) 2173, arXiv:1208.1390 [hep-ex].
- [4] ATLAS Collaboration, Measurements of $W^{\pm}Z$ production cross sections in pp collisions at $\sqrt{s} = 8$ TeV with the ATLAS detector and limits on anomalous gauge boson self-couplings, *Phys. Rev. D* 93 (2016) 092004, arXiv:1603.02151 [hep-ex].
- [5] J. Ohnemus, $\text{Order-}\alpha_s$ calculation of hadronic $W^{\pm}Z$ production, *Phys. Rev. D* 44 (1991) 3477.
- [6] S. Frixione, P. Nason, G. Ridolfi, Strong corrections to WZ production at hadron colliders, *Nucl. Phys. B* 383 (1992) 3.
- [7] M. Grazzini, S. Kallweit, D. Rathlev, M. Wiesemann, $W^{\pm}Z$ production at hadron colliders in NNLO QCD, arXiv:1604.08576 [hep-ph], 2016 (we thank M. Grazzini, S. Kallweit, D. Rathlev and M. Wiesemann for providing the NNLO predictions for the total $W^{\pm}Z$ cross section).
- [8] ATLAS Collaboration, The ATLAS experiment at the CERN Large Hadron Collider, *J. Instrum.* 3 (2008) S08003.
- [9] ATLAS Collaboration, ATLAS insertable B-layer technical design report, CERN-LHCC-2010-013, ATLAS-TDR-19, CERN, 2010, <http://cds.cern.ch/record/1291633>.
- [10] ATLAS Collaboration, ATLAS insertable B-layer technical design report addendum, CERN-LHCC-2012-009, ATLAS-TDR-19-ADD-1, Addendum to CERN-LHCC-2010-013, ATLAS-TDR-019, CERN, 2012, <http://cds.cern.ch/record/1451888>.
- [11] K.A. Olive, et al., Review of particle physics, *Chin. Phys. C* 38 (2014) 090001.
- [12] M. Cacciari, G.P. Salam, G. Soyez, The anti- $k(t)$ jet clustering algorithm, *J. High Energy Phys.* 0804 (2008) 063, arXiv:0802.1189 [hep-ph].
- [13] ATLAS Collaboration, The ATLAS simulation infrastructure, *Eur. Phys. J. C* 70 (2010) 823, arXiv:1005.4568 [physics.ins-det].
- [14] S. Agostinelli, et al., GEANT4: a simulation toolkit, *Nucl. Instrum. Methods A* 506 (2003) 250–303.
- [15] T. Sjöstrand, S. Mrenna, P.Z. Skands, A brief introduction to PYTHIA 8.1, *Comput. Phys. Commun.* 178 (2008) 852, arXiv:0710.3820 [hep-ph].
- [16] A.D. Martin, W.J. Stirling, R.S. Thorne, G. Watt, Parton distributions for the LHC, *Eur. Phys. J. C* 63 (2009) 189, arXiv:0901.0002 [hep-ph].
- [17] ATLAS Collaboration, Summary of ATLAS Pythia 8 Tunes, ATL-PHYS-PUB-2012-003, CERN, 2012, <http://cds.cern.ch/record/1474107>.
- [18] ATLAS Collaboration, Electron identification measurements in ATLAS using $\sqrt{s} = 13$ TeV data with 50 ns bunch spacing, ATL-PHYS-PUB-2015-041, <http://cdsweb.cern.ch/record/2048202>, 2015.
- [19] ATLAS Collaboration, Electron efficiency measurements with the ATLAS detector using the 2012 LHC proton–proton collision data, ATLAS-CONF-2014-032, CERN, 2014, <http://cds.cern.ch/record/1706245>.
- [20] ATLAS Collaboration, Muon reconstruction performance of the ATLAS detector in proton–proton collision data at $\sqrt{s} = 13$ TeV, *Eur. Phys. J. C* 76 (2016) 292, <http://dx.doi.org/10.1140/epjc/s10052-016-4120-y>, arXiv:1603.05598 [hep-ex].

- [21] ATLAS Collaboration, Electron and photon energy calibration with the ATLAS detector using LHC Run 1 data, *Eur. Phys. J. C* 74 (2014) 3071, arXiv:1407.5063 [hep-ex].
- [22] P. Nason, A new method for combining NLO QCD with shower Monte Carlo algorithms, *J. High Energy Phys.* 0411 (2004) 040, arXiv:hep-ph/0409146.
- [23] S. Frixione, P. Nason, C. Oleari, Matching NLO QCD computations with parton shower simulations: the POWHEG method, *J. High Energy Phys.* 0711 (2007) 070, arXiv:0709.2092 [hep-ph].
- [24] S. Alioli, et al., A general framework for implementing NLO calculations in shower Monte Carlo programs: the POWHEG BOX, *J. High Energy Phys.* 1006 (2010) 043, arXiv:1002.2581 [hep-ph].
- [25] T. Melia, et al., W^+W^- , WZ and ZZ production in the POWHEG BOX, *J. High Energy Phys.* 1111 (2011) 078, arXiv:1107.5051 [hep-ph].
- [26] ATLAS Collaboration, Measurement of the Z/γ^* boson transverse momentum distribution in pp collisions at $\sqrt{s} = 7$ TeV with the ATLAS detector, *J. High Energy Phys.* 1409 (2014) 145, arXiv:1406.3660 [hep-ex].
- [27] H.-L. Lai, et al., New parton distributions for collider physics, *Phys. Rev. D* 82 (2010) 074024, arXiv:1007.2241 [hep-ph].
- [28] J. Pumplin, et al., New generation of parton distributions with uncertainties from global QCD analysis, *J. High Energy Phys.* 0207 (2002) 012, arXiv:hep-ph/0201195.
- [29] T. Gleisberg, et al., Event generation with SHERPA 1.1, *J. High Energy Phys.* 0902 (2009) 007, arXiv:0811.4622 [hep-ph].
- [30] S. Schumann, F. Krauss, A parton shower algorithm based on Catani–Seymour dipole factorisation, *J. High Energy Phys.* 0803 (2008) 038, arXiv:0709.1027 [hep-ph].
- [31] T. Sjöstrand, S. Mrenna, P.Z. Skands, PYTHIA 6.4 physics and manual, *J. High Energy Phys.* 0605 (2006) 026, arXiv:hep-ph/0603175.
- [32] P.Z. Skands, Tuning Monte Carlo generators: the perugia tunes, *Phys. Rev. D* 82 (2010) 074018, arXiv:1005.3457 [hep-ph].
- [33] S. Höche, et al., QCD matrix elements and truncated showers, *J. High Energy Phys.* 0905 (2009) 053, arXiv:0903.1219 [hep-ph].
- [34] T. Gleisberg, S. Höche, Comix, a new matrix element generator, *J. High Energy Phys.* 0812 (2008) 039, arXiv:0808.3674 [hep-ph].
- [35] M. Schönherr, F. Krauss, Soft photon radiation in particle decays in SHERPA, *J. High Energy Phys.* 0812 (2008) 018, arXiv:0810.5071 [hep-ph].
- [36] S. Höche, et al., QCD matrix elements + parton showers. The NLO case, *J. High Energy Phys.* 1304 (2013) 027, arXiv:1207.5030 [hep-ph].
- [37] J. Alwall, et al., The automated computation of tree-level and next-to-leading order differential cross sections, and their matching to parton shower simulations, *J. High Energy Phys.* 1407 (2014) 079, arXiv:1405.0301 [hep-ph].
- [38] R.D. Ball, et al., Parton distributions with LHC data, *Nucl. Phys. B* 867 (2013) 244, arXiv:1207.1303 [hep-ph].
- [39] ATLAS Collaboration, 2015 start-up trigger menu and initial performance assessment of the ATLAS trigger using Run-2 data, ATL-DAQ-PUB-2016-001, <http://cds.cern.ch/record/2136007>, 2016.
- [40] ATLAS Collaboration, Topological cell clustering in the ATLAS calorimeters and its performance in LHC Run 1, *Eur. Phys. J. C* (2016), submitted for publication, arXiv:1603.02934 [hep-ex], CERN-PH-EP-2015-304.
- [41] ATLAS Collaboration, Selection of jets produced in 13 TeV proton–proton collisions with the ATLAS detector, ATLAS-CONF-2015-029, <http://cdsweb.cern.ch/record/2037702>, 2015.
- [42] ATLAS Collaboration, Performance of pile-up mitigation techniques for jets in pp collisions at $\sqrt{s} = 8$ TeV using the ATLAS detector, *Nucl. Instrum. Methods A* 824 (2016) 267–370.
- [43] ATLAS Collaboration, Jet calibration and systematic uncertainties for jets reconstructed in the ATLAS detector at $\sqrt{s} = 13$ TeV, ATL-PHYS-PUB-2015-015, <http://cds.cern.ch/record/2037613>, 2015.
- [44] ATLAS Collaboration, Performance of missing transverse momentum reconstruction with the ATLAS detector in the first proton–proton collisions at $\sqrt{s} = 13$ TeV, ATL-PHYS-PUB-2015-027, <http://cdsweb.cern.ch/record/2037904>, 2015.
- [45] F. Cascioli, et al., ZZ production at hadron colliders in NNLO QCD, *Phys. Lett. B* 735 (2014) 311, arXiv:1405.2219 [hep-ph].
- [46] A. Bierweiler, T. Kasprzik, J.H. Kühn, Vector-boson pair production at the LHC to $O(\alpha^3)$ accuracy, *J. High Energy Phys.* 1312 (2013) 071, arXiv:1305.5402 [hep-ph].
- [47] J. Baglio, L.D. Ninh, M.M. Weber, Massive gauge boson pair production at the LHC: a next-to-leading order story, *Phys. Rev. D* 88 (2013) 113005, arXiv:1307.4331.
- [48] F. Caola, et al., QCD corrections to ZZ production in gluon fusion at the LHC, *Phys. Rev. D* 92 (2015) 094028, arXiv:1509.06734 [hep-ph].
- [49] G. D’Agostini, A multidimensional unfolding method based on Bayes’ theorem, *Nucl. Instrum. Methods A* 362 (1995) 487.
- [50] T. Adye, Unfolding algorithms and tests using RooUnfold, in: Proceedings of the PHYSTAT 2011 Workshop, CERN, Geneva, Switzerland, 2011, p. 313, arXiv:1105.1160 [physics.data-an].
- [51] S. Dulat, et al., New parton distribution functions from a global analysis of quantum chromodynamics, *Phys. Rev. D* 93 (2016) 033006, arXiv:1506.07443 [hep-ph].
- [52] L.A. Harland-Lang, et al., Parton distributions in the LHC era: MMHT 2014 PDFs, *Eur. Phys. J. C* 75 (2015) 204, arXiv:1412.3989 [hep-ph].
- [53] R.D. Ball, et al., Parton distributions for the LHC Run II, *J. High Energy Phys.* 1504 (2015) 040, arXiv:1410.8849 [hep-ph].
- [54] J. Butterworth, et al., PDF4LHC recommendations for LHC Run II, *J. Phys. G* 43 (2016) 023001, arXiv:1510.03865 [hep-ph].
- [55] ATLAS Collaboration, Multi-boson simulation for 13 TeV ATLAS analyses, ATL-PHYS-PUB-2016-002, <http://cds.cern.ch/record/2119986>, 2016.
- [56] ATLAS Collaboration, Improved luminosity determination in pp collisions at $\sqrt{s}(s) = 7$ TeV using the ATLAS detector at the LHC, *Eur. Phys. J. C* 73 (2013) 2518, arXiv:1302.4393 [hep-ex].
- [57] ATLAS Collaboration, Luminosity determination in pp collisions at $\sqrt{s} = 8$ TeV using the ATLAS detector at the LHC, *Eur. Phys. J. C* (2016), submitted for publication, arXiv:1608.03953 [hep-ex], CERN-PH-EP-2016-117.
- [58] A. Glazov, Averaging of DIS cross section data, AIP Conf. Proc. 792 (2005) 237.
- [59] H1 Collaboration, F.D. Aaron, et al., Measurement of the inclusive ep scattering cross section at low Q^2 and x at HERA, *Eur. Phys. J. C* 63 (2009) 625, arXiv:0904.0929 [hep-ex].
- [60] H1 Collaboration, ZEUS Collaboration, F.D. Aaron, et al., Combined measurement and QCD analysis of the inclusive ep scattering cross sections at HERA, *J. High Energy Phys.* 1001 (2010) 109, arXiv:0911.0884 [hep-ex].
- [61] ATLAS computing acknowledgements 2016–2017, Tech. rep. ATL-GEN-PUB-2016-002, CERN, 2016, <https://cds.cern.ch/record/2202407>.

ATLAS Collaboration

M. Aaboud^{135d}, G. Aad⁸⁶, B. Abbott¹¹³, J. Abdallah⁶⁴, O. Abidinov¹², B. Abeloos¹¹⁷, R. Aben¹⁰⁷, O.S. AbouZeid¹³⁷, N.L. Abraham¹⁴⁹, H. Abramowicz¹⁵³, H. Abreu¹⁵², R. Abreu¹¹⁶, Y. Abulaiti^{146a,146b}, B.S. Acharya^{163a,163b,a}, L. Adamczyk^{40a}, D.L. Adams²⁷, J. Adelman¹⁰⁸, S. Adomeit¹⁰⁰, T. Adye¹³¹, A.A. Affolder⁷⁵, T. Agatonovic-Jovin¹⁴, J. Agricola⁵⁶, J.A. Aguilar-Saavedra^{126a,126f}, S.P. Ahlen²⁴, F. Ahmadov^{66,b}, G. Aielli^{133a,133b}, H. Akerstedt^{146a,146b}, T.P.A. Åkesson⁸², A.V. Akimov⁹⁶, G.L. Alberghi^{22a,22b}, J. Albert¹⁶⁸, S. Albrand⁵⁷, M.J. Alconada Verzini⁷², M. Aleksa³², I.N. Aleksandrov⁶⁶, C. Alexa^{28b}, G. Alexander¹⁵³, T. Alexopoulos¹⁰, M. Alhroob¹¹³, B. Ali¹²⁸, M. Aliev^{74a,74b}, G. Alimonti^{92a}, J. Alison³³, S.P. Alkire³⁷, B.M.M. Allbrooke¹⁴⁹, B.W. Allen¹¹⁶, P.P. Allport¹⁹, A. Aloisio^{104a,104b}, A. Alonso³⁸, F. Alonso⁷², C. Alpignani¹³⁸, M. Alstady⁸⁶, B. Alvarez Gonzalez³², D. Álvarez Piqueras¹⁶⁶, M.G. Alviggi^{104a,104b}, B.T. Amadio¹⁶, K. Amako⁶⁷, Y. Amaral Coutinho^{26a}, C. Amelung²⁵, D. Amidei⁹⁰, S.P. Amor Dos Santos^{126a,126c}, A. Amorim^{126a,126b}, S. Amoroso³², G. Amundsen²⁵, C. Anastopoulos¹³⁹, L.S. Ancu⁵¹, N. Andari¹⁰⁸, T. Andeen¹¹, C.F. Anders^{59b}, G. Anders³², J.K. Anders⁷⁵, K.J. Anderson³³, A. Andreazza^{92a,92b}, V. Andrei^{59a}, S. Angelidakis⁹, I. Angelozzi¹⁰⁷, P. Anger⁴⁶, A. Angerami³⁷, F. Anghinolfi³², A.V. Anisenkov^{109,c}, N. Anjos¹³, A. Annovi^{124a,124b}, C. Antel^{59a}, M. Antonelli⁴⁹, A. Antonov^{98,*}, F. Anulli^{132a}, M. Aoki⁶⁷, L. Aperio Bella¹⁹, G. Arabidze⁹¹, Y. Arai⁶⁷, J.P. Araque^{126a},

A.T.H. Arce⁴⁷, F.A. Arduh⁷², J-F. Arguin⁹⁵, S. Argyropoulos⁶⁴, M. Arik^{20a}, A.J. Armbruster¹⁴³, L.J. Armitage⁷⁷, O. Arnaez³², H. Arnold⁵⁰, M. Arratia³⁰, O. Arslan²³, A. Artamonov⁹⁷, G. Artoni¹²⁰, S. Artz⁸⁴, S. Asai¹⁵⁵, N. Asbah⁴⁴, A. Ashkenazi¹⁵³, B. Åsman^{146a,146b}, L. Asquith¹⁴⁹, K. Assamagan²⁷, R. Astalos^{144a}, M. Atkinson¹⁶⁵, N.B. Atlay¹⁴¹, K. Augsten¹²⁸, G. Avolio³², B. Axen¹⁶, M.K. Ayoub¹¹⁷, G. Azuelos^{95,d}, M.A. Baak³², A.E. Baas^{59a}, M.J. Baca¹⁹, H. Bachacou¹³⁶, K. Bachas^{74a,74b}, M. Backes³², M. Backhaus³², P. Bagiacchi^{132a,132b}, P. Bagnaia^{132a,132b}, Y. Bai^{35a}, J.T. Baines¹³¹, O.K. Baker¹⁷⁵, E.M. Baldin^{109,c}, P. Balek¹⁷¹, T. Balestri¹⁴⁸, F. Balli¹³⁶, W.K. Balunas¹²², E. Banas⁴¹, Sw. Banerjee^{172,e}, A.A.E. Bannoura¹⁷⁴, L. Barak³², E.L. Barberio⁸⁹, D. Barberis^{52a,52b}, M. Barbero⁸⁶, T. Barillari¹⁰¹, M-S Barisits³², T. Barklow¹⁴³, N. Barlow³⁰, S.L. Barnes⁸⁵, B.M. Barnett¹³¹, R.M. Barnett¹⁶, Z. Barnovska⁵, A. Baroncelli^{134a}, G. Barone²⁵, A.J. Barr¹²⁰, L. Barranco Navarro¹⁶⁶, F. Barreiro⁸³, J. Barreiro Guimarães da Costa^{35a}, R. Bartoldus¹⁴³, A.E. Barton⁷³, P. Bartos^{144a}, A. Basalae¹²³, A. Bassalat¹¹⁷, R.L. Bates⁵⁵, S.J. Batista¹⁵⁸, J.R. Batley³⁰, M. Battaglia¹³⁷, M. Bause^{132a,132b}, F. Bauer¹³⁶, H.S. Bawa^{143,f}, J.B. Beacham¹¹¹, M.D. Beattie⁷³, T. Beau⁸¹, P.H. Beauchemin¹⁶¹, P. Bechtel²³, H.P. Beck^{18,g}, K. Becker¹²⁰, M. Becker⁸⁴, M. Beckingham¹⁶⁹, C. Becot¹¹⁰, A.J. Beddall^{20e}, A. Beddall^{20b}, V.A. Bednyakov⁶⁶, M. Bedognetti¹⁰⁷, C.P. Bee¹⁴⁸, L.J. Beemster¹⁰⁷, T.A. Beermann³², M. Begel²⁷, J.K. Behr⁴⁴, C. Belanger-Champagne⁸⁸, A.S. Bell⁷⁹, G. Bella¹⁵³, L. Bellagamba^{22a}, A. Bellerive³¹, M. Bellomo⁸⁷, K. Belotskiy⁹⁸, O. Beltramello³², N.L. Belyaev⁹⁸, O. Benary¹⁵³, D. Bencheekroun^{135a}, M. Bender¹⁰⁰, K. Bendtz^{146a,146b}, N. Benekos¹⁰, Y. Benhammou¹⁵³, E. Benhar Nocchioli¹⁷⁵, J. Benitez⁶⁴, D.P. Benjamin⁴⁷, J.R. Bensinger²⁵, S. Bentvelsen¹⁰⁷, L. Beresford¹²⁰, M. Beretta⁴⁹, D. Berge¹⁰⁷, E. Bergeaas Kuutmann¹⁶⁴, N. Berger⁵, J. Beringer¹⁶, S. Berlendis⁵⁷, N.R. Bernard⁸⁷, C. Bernius¹¹⁰, F.U. Bernlochner²³, T. Berry⁷⁸, P. Berta¹²⁹, C. Bertella⁸⁴, G. Bertoli^{146a,146b}, F. Bertolucci^{124a,124b}, I.A. Bertram⁷³, C. Bertsche⁴⁴, D. Bertsche¹¹³, G.J. Besjes³⁸, O. Bessidskaia Bylund^{146a,146b}, M. Bessner⁴⁴, N. Besson¹³⁶, C. Betancourt⁵⁰, S. Bethke¹⁰¹, A.J. Bevan⁷⁷, R.M. Bianchi¹²⁵, L. Bianchini²⁵, M. Bianco³², O. Biebel¹⁰⁰, D. Biedermann¹⁷, R. Bielski⁸⁵, N.V. Biesuz^{124a,124b}, M. Biglietti^{134a}, J. Bilbao De Mendizabal⁵¹, T.R.V. Billoud⁹⁵, H. Bilokon⁴⁹, M. Bindi⁵⁶, S. Binet¹¹⁷, A. Bingul^{20b}, C. Bini^{132a,132b}, S. Biondi^{22a,22b}, D.M. Bjergaard⁴⁷, C.W. Black¹⁵⁰, J.E. Black¹⁴³, K.M. Black²⁴, D. Blackburn¹³⁸, R.E. Blair⁶, J.-B. Blanchard¹³⁶, J.E. Blanco⁷⁸, T. Blazek^{144a}, I. Bloch⁴⁴, C. Blocker²⁵, W. Blum^{84,*}, U. Blumenschein⁵⁶, S. Blunier^{34a}, G.J. Bobbink¹⁰⁷, V.S. Bobrovnikov^{109,c}, S.S. Bocchetta⁸², A. Bocci⁴⁷, C. Bock¹⁰⁰, M. Boehler⁵⁰, D. Boerner¹⁷⁴, J.A. Bogaerts³², D. Bogavac¹⁴, A.G. Bogdanchikov¹⁰⁹, C. Bohm^{146a}, V. Boisvert⁷⁸, P. Bokan¹⁴, T. Bold^{40a}, A.S. Boldyrev^{163a,163c}, M. Bomben⁸¹, M. Bona⁷⁷, M. Boonekamp¹³⁶, A. Borisov¹³⁰, G. Borissov⁷³, J. Bortfeldt³², D. Bortoletto¹²⁰, V. Bortolotto^{61a,61b,61c}, K. Bos¹⁰⁷, D. Boscherini^{22a}, M. Bosman¹³, J.D. Bossio Sola²⁹, J. Boudreau¹²⁵, J. Bouffard², E.V. Bouhova-Thacker⁷³, D. Boumediene³⁶, C. Bourdarios¹¹⁷, S.K. Boutle⁵⁵, A. Boveia³², J. Boyd³², I.R. Boyko⁶⁶, J. Bracinik¹⁹, A. Brandt⁸, G. Brandt⁵⁶, O. Brandt^{59a}, U. Bratzler¹⁵⁶, B. Brau⁸⁷, J.E. Brau¹¹⁶, H.M. Braun^{174,*}, W.D. Breaden Madden⁵⁵, K. Brendlinger¹²², A.J. Brennan⁸⁹, L. Brenner¹⁰⁷, R. Brenner¹⁶⁴, S. Bressler¹⁷¹, T.M. Bristow⁴⁸, D. Britton⁵⁵, D. Britzger⁴⁴, F.M. Brochu³⁰, I. Brock²³, R. Brock⁹¹, G. Brooijmans³⁷, T. Brooks⁷⁸, W.K. Brooks^{34b}, J. Brosamer¹⁶, E. Brost¹⁰⁸, J.H. Broughton¹⁹, P.A. Bruckman de Renstrom⁴¹, D. Bruncko^{144b}, R. Bruneliere⁵⁰, A. Bruni^{22a}, G. Bruni^{22a}, L.S. Bruni¹⁰⁷, B.H. Brunt³⁰, M. Bruschi^{22a}, N. Bruscino²³, P. Bryant³³, L. Bryngemark⁸², T. Buanes¹⁵, Q. Buat¹⁴², P. Buchholz¹⁴¹, A.G. Buckley⁵⁵, I.A. Budagov⁶⁶, F. Buehrer⁵⁰, M.K. Bugge¹¹⁹, O. Bulekov⁹⁸, D. Bullock⁸, H. Burckhart³², S. Burdin⁷⁵, C.D. Burgard⁵⁰, B. Burghgrave¹⁰⁸, K. Burka⁴¹, S. Burke¹³¹, I. Burmeister⁴⁵, J.T.P. Burr¹²⁰, E. Busato³⁶, D. Büscher⁵⁰, V. Büscher⁸⁴, P. Bussey⁵⁵, J.M. Butler²⁴, C.M. Buttar⁵⁵, J.M. Butterworth⁷⁹, P. Butti¹⁰⁷, W. Buttinger²⁷, A. Buzatu⁵⁵, A.R. Buzykaev^{109,c}, S. Cabrera Urbán¹⁶⁶, D. Caforio¹²⁸, V.M. Cairo^{39a,39b}, O. Cakir^{4a}, N. Calace⁵¹, P. Calafiura¹⁶, A. Calandri⁸⁶, G. Calderini⁸¹, P. Calfayan¹⁰⁰, G. Callea^{39a,39b}, L.P. Caloba^{26a}, S. Calvente Lopez⁸³, D. Calvet³⁶, S. Calvet³⁶, T.P. Calvet⁸⁶, R. Camacho Toro³³, S. Camarda³², P. Camarri^{133a,133b}, D. Cameron¹¹⁹, R. Caminal Armadans¹⁶⁵, C. Camincher⁵⁷, S. Campana³², M. Campanelli⁷⁹, A. Camplani^{92a,92b}, A. Campoverde¹⁴¹, V. Canale^{104a,104b}, A. Canepa^{159a}, M. Cano Bret^{35e}, J. Cantero¹¹⁴, R. Cantrill^{126a}, T. Cao⁴², M.D.M. Capeans Garrido³², I. Caprini^{28b}, M. Caprini^{28b}, M. Capua^{39a,39b}, R. Caputo⁸⁴, R.M. Carbone³⁷, R. Cardarelli^{133a}, F. Cardillo⁵⁰, I. Carli¹²⁹, T. Carli³², G. Carlino^{104a}, L. Carminati^{92a,92b}, S. Caron¹⁰⁶, E. Carquin^{34b}, G.D. Carrillo-Montoya³², J.R. Carter³⁰, J. Carvalho^{126a,126c}, D. Casadei¹⁹, M.P. Casado^{13,h}, M. Casolino¹³, D.W. Casper¹⁶²,

E. Castaneda-Miranda ^{145a}, R. Castelijns ¹⁰⁷, A. Castelli ¹⁰⁷, V. Castillo Gimenez ¹⁶⁶, N.F. Castro ^{126a,i}, A. Catinaccio ³², J.R. Catmore ¹¹⁹, A. Cattai ³², J. Caudron ⁸⁴, V. Cavaliere ¹⁶⁵, E. Cavallaro ¹³, D. Cavalli ^{92a}, M. Cavalli-Sforza ¹³, V. Cavasinni ^{124a,124b}, F. Ceradini ^{134a,134b}, L. Cerda Alberich ¹⁶⁶, B.C. Cerio ⁴⁷, A.S. Cerqueira ^{26b}, A. Cerri ¹⁴⁹, L. Cerrito ⁷⁷, F. Cerutti ¹⁶, M. Cerv ³², A. Cervelli ¹⁸, S.A. Cetin ^{20d}, A. Chafaq ^{135a}, D. Chakraborty ¹⁰⁸, S.K. Chan ⁵⁸, Y.L. Chan ^{61a}, P. Chang ¹⁶⁵, J.D. Chapman ³⁰, D.G. Charlton ¹⁹, A. Chatterjee ⁵¹, C.C. Chau ¹⁵⁸, C.A. Chavez Barajas ¹⁴⁹, S. Che ¹¹¹, S. Cheatham ⁷³, A. Chegwidden ⁹¹, S. Chekanov ⁶, S.V. Chekulaev ^{159a}, G.A. Chelkov ^{66,j}, M.A. Chelstowska ⁹⁰, C. Chen ⁶⁵, H. Chen ²⁷, K. Chen ¹⁴⁸, S. Chen ^{35c}, S. Chen ¹⁵⁵, X. Chen ^{35f}, Y. Chen ⁶⁸, H.C. Cheng ⁹⁰, H.J. Cheng ^{35a}, Y. Cheng ³³, A. Cheplakov ⁶⁶, E. Cheremushkina ¹³⁰, R. Cherkaoui El Moursli ^{135e}, V. Chernyatin ^{27,*}, E. Cheu ⁷, L. Chevalier ¹³⁶, V. Chiarella ⁴⁹, G. Chiarelli ^{124a,124b}, G. Chiodini ^{74a}, A.S. Chisholm ¹⁹, A. Chitan ^{28b}, M.V. Chizhov ⁶⁶, K. Choi ⁶², A.R. Chomont ³⁶, S. Chouridou ⁹, B.K.B. Chow ¹⁰⁰, V. Christodoulou ⁷⁹, D. Chromek-Burckhart ³², J. Chudoba ¹²⁷, A.J. Chuinard ⁸⁸, J.J. Chwastowski ⁴¹, L. Chytka ¹¹⁵, G. Ciapetti ^{132a,132b}, A.K. Ciftci ^{4a}, D. Cinca ⁴⁵, V. Cindro ⁷⁶, I.A. Cioara ²³, C. Ciocca ^{22a,22b}, A. Ciochio ¹⁶, F. Ciotto ^{104a,104b}, Z.H. Citron ¹⁷¹, M. Citterio ^{92a}, M. Ciubancan ^{28b}, A. Clark ⁵¹, B.L. Clark ⁵⁸, M.R. Clark ³⁷, P.J. Clark ⁴⁸, R.N. Clarke ¹⁶, C. Clement ^{146a,146b}, Y. Coadou ⁸⁶, M. Cobal ^{163a,163c}, A. Coccaro ⁵¹, J. Cochran ⁶⁵, L. Coffey ²⁵, L. Colasurdo ¹⁰⁶, B. Cole ³⁷, A.P. Colijn ¹⁰⁷, J. Collot ⁵⁷, T. Colombo ³², G. Compostella ¹⁰¹, P. Conde Muiño ^{126a,126b}, E. Coniavitis ⁵⁰, S.H. Connell ^{145b}, I.A. Connelly ⁷⁸, V. Consorti ⁵⁰, S. Constantinescu ^{28b}, G. Conti ³², F. Conventi ^{104a,k}, M. Cooke ¹⁶, B.D. Cooper ⁷⁹, A.M. Cooper-Sarkar ¹²⁰, K.J.R. Cormier ¹⁵⁸, T. Cornelissen ¹⁷⁴, M. Corradi ^{132a,132b}, F. Corriveau ^{88,l}, A. Corso-Radu ¹⁶², A. Cortes-Gonzalez ¹³, G. Cortiana ¹⁰¹, G. Costa ^{92a}, M.J. Costa ¹⁶⁶, D. Costanzo ¹³⁹, G. Cottin ³⁰, G. Cowan ⁷⁸, B.E. Cox ⁸⁵, K. Cranmer ¹¹⁰, S.J. Crawley ⁵⁵, G. Cree ³¹, S. Crépé-Renaudin ⁵⁷, F. Crescioli ⁸¹, W.A. Cribbs ^{146a,146b}, M. Crispin Ortuzar ¹²⁰, M. Cristinziani ²³, V. Croft ¹⁰⁶, G. Crosetti ^{39a,39b}, A. Cueto ⁸³, T. Cuhadar Donszelmann ¹³⁹, J. Cummings ¹⁷⁵, M. Curatolo ⁴⁹, J. Cúth ⁸⁴, C. Cuthbert ¹⁵⁰, H. Czirr ¹⁴¹, P. Czodrowski ³, G. D'amen ^{22a,22b}, S. D'Auria ⁵⁵, M. D'Onofrio ⁷⁵, M.J. Da Cunha Sargedas De Sousa ^{126a,126b}, C. Da Via ⁸⁵, W. Dabrowski ^{40a}, T. Dado ^{144a}, T. Dai ⁹⁰, O. Dale ¹⁵, F. Dallaire ⁹⁵, C. Dallapiccola ⁸⁷, M. Dam ³⁸, J.R. Dandoy ³³, N.P. Dang ⁵⁰, A.C. Daniells ¹⁹, N.S. Dann ⁸⁵, M. Danninger ¹⁶⁷, M. Dano Hoffmann ¹³⁶, V. Dao ⁵⁰, G. Darbo ^{52a}, S. Darmora ⁸, J. Dassoulas ³, A. Dattagupta ⁶², W. Davey ²³, C. David ¹⁶⁸, T. Davidek ¹²⁹, M. Davies ¹⁵³, P. Davison ⁷⁹, E. Dawe ⁸⁹, I. Dawson ¹³⁹, R.K. Daya-Ishmukhametova ⁸⁷, K. De ⁸, R. de Asmundis ^{104a}, A. De Benedetti ¹¹³, S. De Castro ^{22a,22b}, S. De Cecco ⁸¹, N. De Groot ¹⁰⁶, P. de Jong ¹⁰⁷, H. De la Torre ⁸³, F. De Lorenzi ⁶⁵, A. De Maria ⁵⁶, D. De Pedis ^{132a}, A. De Salvo ^{132a}, U. De Sanctis ¹⁴⁹, A. De Santo ¹⁴⁹, J.B. De Vivie De Regie ¹¹⁷, W.J. Dearnaley ⁷³, R. Debbe ²⁷, C. Debenedetti ¹³⁷, D.V. Dedovich ⁶⁶, N. Dehghanian ³, I. Deigaard ¹⁰⁷, M. Del Gaudio ^{39a,39b}, J. Del Peso ⁸³, T. Del Prete ^{124a,124b}, D. Delgove ¹¹⁷, F. Deliot ¹³⁶, C.M. Delitzsch ⁵¹, M. Deliyergiyev ⁷⁶, A. Dell'Acqua ³², L. Dell'Asta ²⁴, M. Dell'Orso ^{124a,124b}, M. Della Pietra ^{104a,k}, D. della Volpe ⁵¹, M. Delmastro ⁵, P.A. Delsart ⁵⁷, D.A. DeMarco ¹⁵⁸, S. Demers ¹⁷⁵, M. Demichev ⁶⁶, A. Demilly ⁸¹, S.P. Denisov ¹³⁰, D. Denysiuk ¹³⁶, D. Derendarz ⁴¹, J.E. Derkaoui ^{135d}, F. Derue ⁸¹, P. Dervan ⁷⁵, K. Desch ²³, C. Deterre ⁴⁴, K. Dette ⁴⁵, P.O. Deviveiros ³², A. Dewhurst ¹³¹, S. Dhaliwal ²⁵, A. Di Ciaccio ^{133a,133b}, L. Di Ciaccio ⁵, W.K. Di Clemente ¹²², C. Di Donato ^{132a,132b}, A. Di Girolamo ³², B. Di Girolamo ³², B. Di Micco ^{134a,134b}, R. Di Nardo ³², A. Di Simone ⁵⁰, R. Di Sipio ¹⁵⁸, D. Di Valentino ³¹, C. Diaconu ⁸⁶, M. Diamond ¹⁵⁸, F.A. Dias ⁴⁸, M.A. Diaz ^{34a}, E.B. Diehl ⁹⁰, J. Dietrich ¹⁷, S. Diglio ⁸⁶, A. Dimitrievska ¹⁴, J. Dingfelder ²³, P. Dita ^{28b}, S. Dita ^{28b}, F. Dittus ³², F. Djama ⁸⁶, T. Djobava ^{53b}, J.I. Djuvsland ^{59a}, M.A.B. do Vale ^{26c}, D. Dobos ³², M. Dobre ^{28b}, C. Doglioni ⁸², T. Dohmae ¹⁵⁵, J. Dolejsi ¹²⁹, Z. Dolezal ¹²⁹, B.A. Dolgoshein ^{98,*}, M. Donadelli ^{26d}, S. Donati ^{124a,124b}, P. Dondero ^{121a,121b}, J. Donini ³⁶, J. Dopke ¹³¹, A. Doria ^{104a}, M.T. Dova ⁷², A.T. Doyle ⁵⁵, E. Drechsler ⁵⁶, M. Dris ¹⁰, Y. Du ^{35d}, J. Duarte-Campderros ¹⁵³, E. Duchovni ¹⁷¹, G. Duckeck ¹⁰⁰, O.A. Ducu ^{95,m}, D. Duda ¹⁰⁷, A. Dudarev ³², E.M. Duffield ¹⁶, L. Duflost ¹¹⁷, L. Duguid ⁷⁸, M. Dührssen ³², M. Dumancic ¹⁷¹, M. Dunford ^{59a}, H. Duran Yildiz ^{4a}, M. Düren ⁵⁴, A. Durglishvili ^{53b}, D. Duschinger ⁴⁶, B. Dutta ⁴⁴, M. Dyndal ⁴⁴, C. Eckardt ⁴⁴, K.M. Ecker ¹⁰¹, R.C. Edgar ⁹⁰, N.C. Edwards ⁴⁸, T. Eifert ³², G. Eigen ¹⁵, K. Einsweiler ¹⁶, T. Ekelof ¹⁶⁴, M. El Kacimi ^{135c}, V. Ellajosyula ⁸⁶, M. Ellert ¹⁶⁴, S. Elles ⁵, F. Ellinghaus ¹⁷⁴, A.A. Elliot ¹⁶⁸, N. Ellis ³², J. Elmsheuser ²⁷, M. Elsing ³², D. Emelianov ¹³¹, Y. Enari ¹⁵⁵, O.C. Endner ⁸⁴, M. Endo ¹¹⁸, J.S. Ennis ¹⁶⁹, J. Erdmann ⁴⁵, A. Ereditato ¹⁸, G. Ernis ¹⁷⁴, J. Ernst ², M. Ernst ²⁷, S. Errede ¹⁶⁵, E. Ertel ⁸⁴, M. Escalier ¹¹⁷, H. Esch ⁴⁵, C. Escobar ¹²⁵, B. Esposito ⁴⁹, A.I. Etienvre ¹³⁶, E. Etzion ¹⁵³,

H. Evans⁶², A. Ezhilov¹²³, F. Fabbri^{22a,22b}, L. Fabbri^{22a,22b}, G. Facini³³, R.M. Fakhruddinov¹³⁰, S. Falciano^{132a}, R.J. Falla⁷⁹, J. Faltova³², Y. Fang^{35a}, M. Fanti^{92a,92b}, A. Farbin⁸, A. Farilla^{134a}, C. Farina¹²⁵, E.M. Farina^{121a,121b}, T. Farooque¹³, S. Farrell¹⁶, S.M. Farrington¹⁶⁹, P. Farthouat³², F. Fassi^{135e}, P. Fassnacht³², D. Fassouliotis⁹, M. Fauci Giannelli⁷⁸, A. Favareto^{52a,52b}, W.J. Fawcett¹²⁰, L. Fayard¹¹⁷, O.L. Fedin^{123,n}, W. Fedorko¹⁶⁷, S. Feigl¹¹⁹, L. Feligioni⁸⁶, C. Feng^{35d}, E.J. Feng³², H. Feng⁹⁰, A.B. Fenyuk¹³⁰, L. Feremenga⁸, P. Fernandez Martinez¹⁶⁶, S. Fernandez Perez¹³, J. Ferrando⁵⁵, A. Ferrari¹⁶⁴, P. Ferrari¹⁰⁷, R. Ferrari^{121a}, D.E. Ferreira de Lima^{59b}, A. Ferrer¹⁶⁶, D. Ferrere⁵¹, C. Ferretti⁹⁰, A. Ferretto Parodi^{52a,52b}, F. Fiedler⁸⁴, A. Filipčič⁷⁶, M. Filipuzzi⁴⁴, F. Filthaut¹⁰⁶, M. Fincke-Keeler¹⁶⁸, K.D. Finelli¹⁵⁰, M.C.N. Fiolhais^{126a,126c}, L. Fiorini¹⁶⁶, A. Firan⁴², A. Fischer², C. Fischer¹³, J. Fischer¹⁷⁴, W.C. Fisher⁹¹, N. Flaschel⁴⁴, I. Fleck¹⁴¹, P. Fleischmann⁹⁰, G.T. Fletcher¹³⁹, R.R.M. Fletcher¹²², T. Flick¹⁷⁴, A. Floderus⁸², L.R. Flores Castillo^{61a}, M.J. Flowerdew¹⁰¹, G.T. Forcolin⁸⁵, A. Formica¹³⁶, A. Forti⁸⁵, A.G. Foster¹⁹, D. Fournier¹¹⁷, H. Fox⁷³, S. Fracchia¹³, P. Francavilla⁸¹, M. Franchini^{22a,22b}, D. Francis³², L. Franconi¹¹⁹, M. Franklin⁵⁸, M. Frate¹⁶², M. Fraternali^{121a,121b}, D. Freeborn⁷⁹, S.M. Fressard-Batraneanu³², F. Friedrich⁴⁶, D. Froidevaux³², J.A. Frost¹²⁰, C. Fukunaga¹⁵⁶, E. Fullana Torregrosa⁸⁴, T. Fusayasu¹⁰², J. Fuster¹⁶⁶, C. Gabaldon⁵⁷, O. Gabizon¹⁷⁴, A. Gabrielli^{22a,22b}, A. Gabrielli¹⁶, G.P. Gach^{40a}, S. Gadatsch³², S. Gadomski⁵¹, G. Gagliardi^{52a,52b}, L.G. Gagnon⁹⁵, P. Gagnon⁶², C. Galea¹⁰⁶, B. Galhardo^{126a,126c}, E.J. Gallas¹²⁰, B.J. Gallop¹³¹, P. Gallus¹²⁸, G. Galster³⁸, K.K. Gan¹¹¹, J. Gao^{35b,86}, Y. Gao⁴⁸, Y.S. Gao^{143,f}, F.M. Garay Walls⁴⁸, C. García¹⁶⁶, J.E. García Navarro¹⁶⁶, M. Garcia-Sciveres¹⁶, R.W. Gardner³³, N. Garelli¹⁴³, V. Garonne¹¹⁹, A. Gascon Bravo⁴⁴, C. Gatti⁴⁹, A. Gaudiello^{52a,52b}, G. Gaudio^{121a}, B. Gaur¹⁴¹, L. Gauthier⁹⁵, I.L. Gavrilenko⁹⁶, C. Gay¹⁶⁷, G. Gaycken²³, E.N. Gazis¹⁰, Z. Gece¹⁶⁷, C.N.P. Gee¹³¹, Ch. Geich-Gimbel²³, M. Geisen⁸⁴, M.P. Geisler^{59a}, C. Gemme^{52a}, M.H. Genest⁵⁷, C. Geng^{35b,o}, S. Gentile^{132a,132b}, C. Gentsos¹⁵⁴, S. George⁷⁸, D. Gerbaudo¹³, A. Gershon¹⁵³, S. Ghasemi¹⁴¹, H. Ghazlane^{135b}, M. Ghneimat²³, B. Giacobbe^{22a}, S. Giagu^{132a,132b}, P. Giannetti^{124a,124b}, B. Gibbard²⁷, S.M. Gibson⁷⁸, M. Gignac¹⁶⁷, M. Gilchriese¹⁶, T.P.S. Gillam³⁰, D. Gillberg³¹, G. Gilles¹⁷⁴, D.M. Gingrich^{3,d}, N. Giokaris⁹, M.P. Giordani^{163a,163c}, F.M. Giorgi^{22a}, F.M. Giorgi¹⁷, P.F. Giraud¹³⁶, P. Giromini⁵⁸, D. Giugni^{92a}, F. Giuli¹²⁰, C. Giuliani¹⁰¹, M. Giulini^{59b}, B.K. Gjeltsten¹¹⁹, S. Gkaitatzis¹⁵⁴, I. Gkialas¹⁵⁴, E.L. Gkougkousis¹¹⁷, L.K. Gladilin⁹⁹, C. Glasman⁸³, J. Glatzer⁵⁰, P.C.F. Glaysher⁴⁸, A. Glazov⁴⁴, M. Goblirsch-Kolb²⁵, J. Godlewski⁴¹, S. Goldfarb⁸⁹, T. Golling⁵¹, D. Golubkov¹³⁰, A. Gomes^{126a,126b,126d}, R. Gonçalo^{126a}, J. Goncalves Pinto Firmino Da Costa¹³⁶, G. Gonella⁵⁰, L. Gonella¹⁹, A. Gongadze⁶⁶, S. González de la Hoz¹⁶⁶, G. Gonzalez Parra¹³, S. Gonzalez-Sevilla⁵¹, L. Goossens³², P.A. Gorbounov⁹⁷, H.A. Gordon²⁷, I. Gorelov¹⁰⁵, B. Gorini³², E. Gorini^{74a,74b}, A. Gorišek⁷⁶, E. Gornicki⁴¹, A.T. Goshaw⁴⁷, C. Gössling⁴⁵, M.I. Gostkin⁶⁶, C.R. Goudet¹¹⁷, D. Goujdami^{135c}, A.G. Goussiou¹³⁸, N. Govender^{145b,p}, E. Gozani¹⁵², L. Graber⁵⁶, I. Grabowska-Bold^{40a}, P.O.J. Gradin⁵⁷, P. Grafström^{22a,22b}, J. Gramling⁵¹, E. Gramstad¹¹⁹, S. Grancagnolo¹⁷, V. Gratchev¹²³, P.M. Gravila^{28e}, H.M. Gray³², E. Graziani^{134a}, Z.D. Greenwood^{80,q}, C. Grefe²³, K. Gregersen⁷⁹, I.M. Gregor⁴⁴, P. Grenier¹⁴³, K. Grevtsov⁵, J. Griffiths⁸, A.A. Grillo¹³⁷, K. Grimm⁷³, S. Grinstein^{13,r}, Ph. Gris³⁶, J.-F. Grivaz¹¹⁷, S. Groh⁸⁴, J.P. Grohs⁴⁶, E. Gross¹⁷¹, J. Grosse-Knetter⁵⁶, G.C. Grossi⁸⁰, Z.J. Grout¹⁴⁹, L. Guan⁹⁰, W. Guan¹⁷², J. Guenther⁶³, F. Guescini⁵¹, D. Guest¹⁶², O. Gueta¹⁵³, E. Guido^{52a,52b}, T. Guillemain⁵, S. Guindon², U. Gul⁵⁵, C. Gumpert³², J. Guo^{35e}, Y. Guo^{35b,o}, R. Gupta⁴², S. Gupta¹²⁰, G. Gustavino^{132a,132b}, P. Gutierrez¹¹³, N.G. Gutierrez Ortiz⁷⁹, C. Gutsche⁴⁶, C. Guyot¹³⁶, C. Gwenlan¹²⁰, C.B. Gwilliam⁷⁵, A. Haas¹¹⁰, C. Haber¹⁶, H.K. Hadavand⁸, N. Haddad^{135e}, A. Hadeef⁸⁶, P. Haefner²³, S. Hageböck²³, Z. Hajduk⁴¹, H. Hakobyan^{176,*}, M. Haleem⁴⁴, J. Haley¹¹⁴, G. Halladjian⁹¹, G.D. Hallewell⁸⁶, K. Hamacher¹⁷⁴, P. Hamal¹¹⁵, K. Hamano¹⁶⁸, A. Hamilton^{145a}, G.N. Hamity¹³⁹, P.G. Hamnett⁴⁴, L. Han^{35b}, K. Hanagaki^{67,s}, K. Hanawa¹⁵⁵, M. Hance¹³⁷, B. Haney¹²², S. Hanisch³², P. Hanke^{59a}, R. Hanna¹³⁶, J.B. Hansen³⁸, J.D. Hansen³⁸, M.C. Hansen²³, P.H. Hansen³⁸, K. Hara¹⁶⁰, A.S. Hard¹⁷², T. Harenberg¹⁷⁴, F. Hariri¹¹⁷, S. Harkusha⁹³, R.D. Harrington⁴⁸, P.F. Harrison¹⁶⁹, F. Hartjes¹⁰⁷, N.M. Hartmann¹⁰⁰, M. Hasegawa⁶⁸, Y. Hasegawa¹⁴⁰, A. Hasib¹¹³, S. Hassani¹³⁶, S. Haug¹⁸, R. Hauser⁹¹, L. Hauswald⁴⁶, M. Havranek¹²⁷, C.M. Hawkes¹⁹, R.J. Hawking³², D. Hayden⁹¹, C.P. Hays¹²⁰, J.M. Hays⁷⁷, H.S. Hayward⁷⁵, S.J. Haywood¹³¹, S.J. Head¹⁹, T. Heck⁸⁴, V. Hedberg⁸², L. Heelan⁸, S. Heim¹²², T. Heim¹⁶, B. Heinemann¹⁶, J.J. Heinrich¹⁰⁰, L. Heinrich¹¹⁰, C. Heinz⁵⁴, J. Hejbal¹²⁷, L. Helary²⁴, S. Hellman^{146a,146b}, C. Helsens³², J. Henderson¹²⁰, R.C.W. Henderson⁷³, Y. Heng¹⁷², S. Henkelmann¹⁶⁷,

A.M. Henriques Correia³², S. Henrot-Versille¹¹⁷, G.H. Herbert¹⁷, Y. Hernández Jiménez¹⁶⁶, G. Herten⁵⁰, R. Hertenberger¹⁰⁰, L. Hervas³², G.G. Hesketh⁷⁹, N.P. Hessey¹⁰⁷, J.W. Hetherly⁴², R. Hickling⁷⁷, E. Higón-Rodríguez¹⁶⁶, E. Hill¹⁶⁸, J.C. Hill³⁰, K.H. Hiller⁴⁴, S.J. Hillier¹⁹, I. Hinchliffe¹⁶, E. Hines¹²², R.R. Hinman¹⁶, M. Hirose⁵⁰, D. Hirschbuehl¹⁷⁴, J. Hobbs¹⁴⁸, N. Hod^{159a}, M.C. Hodgkinson¹³⁹, P. Hodgson¹³⁹, A. Hoecker³², M.R. Hoferkamp¹⁰⁵, F. Hoenig¹⁰⁰, D. Hohn²³, T.R. Holmes¹⁶, M. Homann⁴⁵, T.M. Hong¹²⁵, B.H. Hooberman¹⁶⁵, W.H. Hopkins¹¹⁶, Y. Horii¹⁰³, A.J. Horton¹⁴², J.-Y. Hostachy⁵⁷, S. Hou¹⁵¹, A. Hoummada^{135a}, J. Howarth⁴⁴, M. Hrabovsky¹¹⁵, I. Hristova¹⁷, J. Hrivnac¹¹⁷, T. Hryn'ova⁵, A. Hrynevich⁹⁴, C. Hsu^{145c}, P.J. Hsu^{151,t}, S.-C. Hsu¹³⁸, D. Hu³⁷, Q. Hu^{35b}, Y. Huang⁴⁴, Z. Hubacek¹²⁸, F. Hubaut⁸⁶, F. Huegging²³, T.B. Huffman¹²⁰, E.W. Hughes³⁷, G. Hughes⁷³, M. Huhtinen³², P. Huo¹⁴⁸, N. Huseynov^{66,b}, J. Huston⁹¹, J. Huth⁵⁸, G. Iacobucci⁵¹, G. Iakovidis²⁷, I. Ibragimov¹⁴¹, L. Iconomidou-Fayard¹¹⁷, E. Ideal¹⁷⁵, Z. Idrissi^{135e}, P. Iengo³², O. Igonkina^{107,u}, T. Iizawa¹⁷⁰, Y. Ikegami⁶⁷, M. Ikeno⁶⁷, Y. Ilchenko^{11,v}, D. Iliadis¹⁵⁴, N. Ilic¹⁴³, T. Ince¹⁰¹, G. Introzzi^{121a,121b}, P. Ioannou^{9,*}, M. Iodice^{134a}, K. Iordanidou³⁷, V. Ippolito⁵⁸, N. Ishijima¹¹⁸, M. Ishino⁶⁹, M. Ishitsuka¹⁵⁷, R. Ishmukhametov¹¹¹, C. Issever¹²⁰, S. Istin^{20a}, F. Ito¹⁶⁰, J.M. Iturbe Ponce⁸⁵, R. Iuppa^{133a,133b}, W. Iwanski⁴¹, H. Iwasaki⁶⁷, J.M. Izen⁴³, V. Izzo^{104a}, S. Jabbar³, B. Jackson¹²², M. Jackson⁷⁵, P. Jackson¹, V. Jain², K.B. Jakobi⁸⁴, K. Jakobs⁵⁰, S. Jakobsen³², T. Jakoubek¹²⁷, D.O. Jamin¹¹⁴, D.K. Jana⁸⁰, E. Jansen⁷⁹, R. Jansky⁶³, J. Janssen²³, M. Janus⁵⁶, G. Jarlskog⁸², N. Javadov^{66,b}, T. Javůrek⁵⁰, F. Jeanneau¹³⁶, L. Jeanty¹⁶, J. Jejelava^{53a,w}, G.-Y. Jeng¹⁵⁰, D. Jennens⁸⁹, P. Jenni^{50,x}, J. Jentzsch⁴⁵, C. Jeske¹⁶⁹, S. Jézéquel⁵, H. Ji¹⁷², J. Jia¹⁴⁸, H. Jiang⁶⁵, Y. Jiang^{35b}, S. Jiggins⁷⁹, J. Jimenez Pena¹⁶⁶, S. Jin^{35a}, A. Jinaru^{28b}, O. Jinnouchi¹⁵⁷, P. Johansson¹³⁹, K.A. Johns⁷, W.J. Johnson¹³⁸, K. Jon-And^{146a,146b}, G. Jones¹⁶⁹, R.W.L. Jones⁷³, S. Jones⁷, T.J. Jones⁷⁵, J. Jongmanns^{59a}, P.M. Jorge^{126a,126b}, J. Jovicevic^{159a}, X. Ju¹⁷², A. Juste Rozas^{13,r}, M.K. Köhler¹⁷¹, A. Kaczmarska⁴¹, M. Kado¹¹⁷, H. Kagan¹¹¹, M. Kagan¹⁴³, S.J. Kahn⁸⁶, E. Kajomovitz⁴⁷, C.W. Kalderon¹²⁰, A. Kaluza⁸⁴, S. Kama⁴², A. Kamenshchikov¹³⁰, N. Kanaya¹⁵⁵, S. Kaneti³⁰, L. Kanjir⁷⁶, V.A. Kantserov⁹⁸, J. Kanzaki⁶⁷, B. Kaplan¹¹⁰, L.S. Kaplan¹⁷², A. Kapliy³³, D. Kar^{145c}, K. Karakostas¹⁰, A. Karamaoun³, N. Karastathis¹⁰, M.J. Kareem⁵⁶, E. Karentzos¹⁰, M. Karnevskiy⁸⁴, S.N. Karpov⁶⁶, Z.M. Karpova⁶⁶, K. Karthik¹¹⁰, V. Kartvelishvili⁷³, A.N. Karyukhin¹³⁰, K. Kasahara¹⁶⁰, L. Kashif¹⁷², R.D. Kass¹¹¹, A. Kastanas¹⁵, Y. Kataoka¹⁵⁵, C. Kato¹⁵⁵, A. Katre⁵¹, J. Katzy⁴⁴, K. Kawagoe⁷¹, T. Kawamoto¹⁵⁵, G. Kawamura⁵⁶, S. Kazama¹⁵⁵, V.F. Kazanin^{109,c}, R. Keeler¹⁶⁸, R. Kehoe⁴², J.S. Keller⁴⁴, J.J. Kempster⁷⁸, K. Kentaro¹⁰³, H. Keoshkerian¹⁵⁸, O. Kepka¹²⁷, B.P. Kerševan⁷⁶, S. Kersten¹⁷⁴, R.A. Keyes⁸⁸, M. Khader¹⁶⁵, F. Khalil-zada¹², A. Khanov¹¹⁴, A.G. Kharlamov^{109,c}, T.J. Khoo⁵¹, V. Khovanskiy⁹⁷, E. Khramov⁶⁶, J. Khubua^{53b,y}, S. Kido⁶⁸, H.Y. Kim⁸, S.H. Kim¹⁶⁰, Y.K. Kim³³, N. Kimura¹⁵⁴, O.M. Kind¹⁷, B.T. King⁷⁵, M. King¹⁶⁶, S.B. King¹⁶⁷, J. Kirk¹³¹, A.E. Kiryunin¹⁰¹, T. Kishimoto⁶⁸, D. Kisiielewska^{40a}, F. Kiss⁵⁰, K. Kiuchi¹⁶⁰, O. Kivernyk¹³⁶, E. Kladiva^{144b}, M.H. Klein³⁷, M. Klein⁷⁵, U. Klein⁷⁵, K. Kleinknecht⁸⁴, P. Klimek¹⁰⁸, A. Klimentov²⁷, R. Klingenberg⁴⁵, J.A. Klinger¹³⁹, T. Klioutchnikova³², E.-E. Kluge^{59a}, P. Kluit¹⁰⁷, S. Kluth¹⁰¹, J. Knapik⁴¹, E. Kneringer⁶³, E.B.F.G. Knoops⁸⁶, A. Knue⁵⁵, A. Kobayashi¹⁵⁵, D. Kobayashi¹⁵⁷, T. Kobayashi¹⁵⁵, M. Kobel⁴⁶, M. Kocian¹⁴³, P. Kodys¹²⁹, T. Koffas³¹, E. Koffeman¹⁰⁷, T. Koi¹⁴³, H. Kolanoski¹⁷, M. Kolb^{59b}, I. Koletsou⁵, A.A. Komar^{96,*}, Y. Komori¹⁵⁵, T. Kondo⁶⁷, N. Kondrashova⁴⁴, K. Köneke⁵⁰, A.C. König¹⁰⁶, T. Kono^{67,z}, R. Konoplich^{110,aa}, N. Konstantinidis⁷⁹, R. Kopeliansky⁶², S. Koperny^{40a}, L. Köpke⁸⁴, A.K. Kopp⁵⁰, K. Korcyl⁴¹, K. Kordas¹⁵⁴, A. Korn⁷⁹, A.A. Korol^{109,c}, I. Korolkov¹³, E.V. Korolkova¹³⁹, O. Kortner¹⁰¹, S. Kortner¹⁰¹, T. Kosek¹²⁹, V.V. Kostyukhin²³, A. Kotwal⁴⁷, A. Kourkouveli-Charalampidi¹⁵⁴, C. Kourkouvelis⁹, V. Kouskoura²⁷, A.B. Kowalewska⁴¹, R. Kowalewski¹⁶⁸, T.Z. Kowalski^{40a}, C. Kozakai¹⁵⁵, W. Kozanecki¹³⁶, A.S. Kozhin¹³⁰, V.A. Kramarenko⁹⁹, G. Kramberger⁷⁶, D. Krasnopevtsev⁹⁸, M.W. Krasny⁸¹, A. Krasznahorkay³², J.K. Kraus²³, A. Kravchenko²⁷, M. Kretz^{59c}, J. Kretzschmar⁷⁵, K. Kreutzfeldt⁵⁴, P. Krieger¹⁵⁸, K. Krizka³³, K. Kroeninger⁴⁵, H. Kroha¹⁰¹, J. Kroll¹²², J. Kroseberg²³, J. Krstic¹⁴, U. Kruchonak⁶⁶, H. Krüger²³, N. Krumnack⁶⁵, A. Kruse¹⁷², M.C. Kruse⁴⁷, M. Kruskal²⁴, T. Kubota⁸⁹, H. Kucuk⁷⁹, S. Kuday^{4b}, J.T. Kuechler¹⁷⁴, S. Kuehn⁵⁰, A. Kugel^{59c}, F. Kuger¹⁷³, A. Kuhl¹³⁷, T. Kuhl⁴⁴, V. Kukhtin⁶⁶, R. Kukla¹³⁶, Y. Kulchitsky⁹³, S. Kuleshov^{34b}, M. Kuna^{132a,132b}, T. Kunigo⁶⁹, A. Kupco¹²⁷, H. Kurashige⁶⁸, Y.A. Kurochkin⁹³, V. Kus¹²⁷, E.S. Kuwertz¹⁶⁸, M. Kuze¹⁵⁷, J. Kvita¹¹⁵, T. Kwan¹⁶⁸, D. Kyriazopoulos¹³⁹, A. La Rosa¹⁰¹, J.L. La Rosa Navarro^{26d}, L. La Rotonda^{39a,39b}, C. Lacasta¹⁶⁶, F. Lacava^{132a,132b}, J. Lacey³¹,

H. Lacker¹⁷, D. Lacour⁸¹, V.R. Lacuesta¹⁶⁶, E. Ladygin⁶⁶, R. Lafaye⁵, B. Laforge⁸¹, T. Lagouri¹⁷⁵, S. Lai⁵⁶, S. Lammers⁶², W. Lampl⁷, E. Lançon¹³⁶, U. Landgraf⁵⁰, M.P.J. Landon⁷⁷, M.C. Lanfermann⁵¹, V.S. Lang^{59a}, J.C. Lange¹³, A.J. Lankford¹⁶², F. Lanni²⁷, K. Lantsch²³, A. Lanza^{121a}, S. Laplace⁸¹, C. Lapoire³², J.F. Laporte¹³⁶, T. Lari^{92a}, F. Lasagni Manghi^{22a,22b}, M. Lassnig³², P. Laurelli⁴⁹, W. Lavrijsen¹⁶, A.T. Law¹³⁷, P. Laycock⁷⁵, T. Lazovich⁵⁸, M. Lazzaroni^{92a,92b}, B. Le⁸⁹, O. Le Dortz⁸¹, E. Le Guirriec⁸⁶, E.P. Le Quilleuc¹³⁶, M. LeBlanc¹⁶⁸, T. LeCompte⁶, F. Ledroit-Guillon⁵⁷, C.A. Lee²⁷, S.C. Lee¹⁵¹, L. Lee¹, G. Lefebvre⁸¹, M. Lefebvre¹⁶⁸, F. Legger¹⁰⁰, C. Leggett¹⁶, A. Lehan⁷⁵, G. Lehmann Miotto³², X. Lei⁷, W.A. Leight³¹, A. Leisos^{154,ab}, A.G. Leister¹⁷⁵, M.A.L. Leite^{26d}, R. Leitner¹²⁹, D. Lellouch¹⁷¹, B. Lemmer⁵⁶, K.J.C. Leney⁷⁹, T. Lenz²³, B. Lenzi³², R. Leone⁷, S. Leone^{124a,124b}, C. Leonidopoulos⁴⁸, S. Leontsinis¹⁰, G. Lerner¹⁴⁹, C. Leroy⁹⁵, A.A.J. Lesage¹³⁶, C.G. Lester³⁰, M. Levchenko¹²³, J. Levêque⁵, D. Levin⁹⁰, L.J. Levinson¹⁷¹, M. Levy¹⁹, D. Lewis⁷⁷, A.M. Leyko²³, M. Leyton⁴³, B. Li^{35b,o}, H. Li¹⁴⁸, H.L. Li³³, L. Li⁴⁷, L. Li^{35e}, Q. Li^{35a}, S. Li⁴⁷, X. Li⁸⁵, Y. Li¹⁴¹, Z. Liang^{35a}, B. Liberti^{133a}, A. Liblong¹⁵⁸, P. Lichard³², K. Lie¹⁶⁵, J. Liebal²³, W. Liebig¹⁵, A. Limosani¹⁵⁰, S.C. Lin^{151,ac}, T.H. Lin⁸⁴, B.E. Lindquist¹⁴⁸, A.E. Lioni⁵¹, E. Lipeles¹²², A. Lipniacka¹⁵, M. Lisovyi^{59b}, T.M. Liss¹⁶⁵, A. Lister¹⁶⁷, A.M. Litke¹³⁷, B. Liu^{151,ad}, D. Liu¹⁵¹, H. Liu⁹⁰, H. Liu²⁷, J. Liu⁸⁶, J.B. Liu^{35b}, K. Liu⁸⁶, L. Liu¹⁶⁵, M. Liu⁴⁷, M. Liu^{35b}, Y.L. Liu^{35b}, Y. Liu^{35b}, M. Livan^{121a,121b}, A. Lleres⁵⁷, J. Llorente Merino^{35a}, S.L. Lloyd⁷⁷, F. Lo Sterzo¹⁵¹, E. Lobodzinska⁴⁴, P. Loch⁷, W.S. Lockman¹³⁷, F.K. Loebinger⁸⁵, A.E. Loevschall-Jensen³⁸, K.M. Loew²⁵, A. Loginov^{175,*}, T. Lohse¹⁷, K. Lohwasser⁴⁴, M. Lokajicek¹²⁷, B.A. Long²⁴, J.D. Long¹⁶⁵, R.E. Long⁷³, L. Longo^{74a,74b}, K.A. Looper¹¹¹, L. Lopes^{126a}, D. Lopez Mateos⁵⁸, B. Lopez Paredes¹³⁹, I. Lopez Paz¹³, A. Lopez Solis⁸¹, J. Lorenz¹⁰⁰, N. Lorenzo Martinez⁶², M. Losada²¹, P.J. Lösel¹⁰⁰, X. Lou^{35a}, A. Lounis¹¹⁷, J. Love⁶, P.A. Love⁷³, H. Lu^{61a}, N. Lu⁹⁰, H.J. Lubatti¹³⁸, C. Luci^{132a,132b}, A. Lucotte⁵⁷, C. Luedtke⁵⁰, F. Luehring⁶², W. Lukas⁶³, L. Luminari^{132a}, O. Lundberg^{146a,146b}, B. Lund-Jensen¹⁴⁷, P.M. Luzi⁸¹, D. Lynn²⁷, R. Lysak¹²⁷, E. Lytken⁸², V. Lyubushkin⁶⁶, H. Ma²⁷, L.L. Ma^{35d}, Y. Ma^{35d}, G. Maccarrone⁴⁹, A. Macchiolo¹⁰¹, C.M. Macdonald¹³⁹, B. Maček⁷⁶, J. Machado Miguens^{122,126b}, D. Madaffari⁸⁶, R. Madar³⁶, H.J. Maddocks¹⁶⁴, W.F. Mader⁴⁶, A. Madsen⁴⁴, J. Maeda⁶⁸, S. Maeland¹⁵, T. Maeno²⁷, A. Maevskiy⁹⁹, E. Magradze⁵⁶, J. Mahlstedt¹⁰⁷, C. Maiani¹¹⁷, C. Maidantchik^{26a}, A.A. Maier¹⁰¹, T. Maier¹⁰⁰, A. Maio^{126a,126b,126d}, S. Majewski¹¹⁶, Y. Makida⁶⁷, N. Makovec¹¹⁷, B. Malaescu⁸¹, Pa. Malecki⁴¹, V.P. Maleev¹²³, F. Malek⁵⁷, U. Mallik⁶⁴, D. Malon⁶, C. Malone¹⁴³, S. Maltezos¹⁰, S. Malyukov³², J. Mamuzic¹⁶⁶, G. Mancini⁴⁹, B. Mandelli³², L. Mandelli^{92a}, I. Mandić⁷⁶, J. Maneira^{126a,126b}, L. Manhaes de Andrade Filho^{26b}, J. Manjarres Ramos^{159b}, A. Mann¹⁰⁰, A. Manousos³², B. Mansoulie¹³⁶, J.D. Mansour^{35a}, R. Mantifel⁸⁸, M. Mantoani⁵⁶, S. Manzoni^{92a,92b}, L. Mapelli³², G. Marceca²⁹, L. March⁵¹, G. Marchiori⁸¹, M. Marcisovsky¹²⁷, M. Marjanovic¹⁴, D.E. Marley⁹⁰, F. Marroquim^{26a}, S.P. Marsden⁸⁵, Z. Marshall¹⁶, S. Marti-Garcia¹⁶⁶, B. Martin⁹¹, T.A. Martin¹⁶⁹, V.J. Martin⁴⁸, B. Martin dit Latour¹⁵, M. Martinez^{13,r}, V.I. Martinez Outschoorn¹⁶⁵, S. Martin-Haugh¹³¹, V.S. Martoiu^{28b}, A.C. Martyniuk⁷⁹, M. Marx¹³⁸, A. Marzin³², L. Masetti⁸⁴, T. Mashimo¹⁵⁵, R. Mashinistov⁹⁶, J. Masik⁸⁵, A.L. Maslennikov^{109,c}, I. Massa^{22a,22b}, L. Massa^{22a,22b}, P. Mastrandrea⁵, A. Mastroberardino^{39a,39b}, T. Masubuchi¹⁵⁵, P. Mättig¹⁷⁴, J. Mattmann⁸⁴, J. Maurer^{28b}, S.J. Maxfield⁷⁵, D.A. Maximov^{109,c}, R. Mazini¹⁵¹, S.M. Mazza^{92a,92b}, N.C. Mc Fadden¹⁰⁵, G. Mc Goldrick¹⁵⁸, S.P. Mc Kee⁹⁰, A. McCarn⁹⁰, R.L. McCarthy¹⁴⁸, T.G. McCarthy¹⁰¹, L.I. McClymont⁷⁹, E.F. McDonald⁸⁹, J.A. Mcfayden⁷⁹, G. Mchedlidze⁵⁶, S.J. McMahon¹³¹, R.A. McPherson^{168,l}, M. Medinnis⁴⁴, S. Meehan¹³⁸, S. Mehlhase¹⁰⁰, A. Mehta⁷⁵, K. Meier^{59a}, C. Meineck¹⁰⁰, B. Meirose⁴³, D. Melini¹⁶⁶, B.R. Mellado Garcia^{145c}, M. Melo^{144a}, F. Meloni¹⁸, A. Mengarelli^{22a,22b}, S. Menke¹⁰¹, E. Meoni¹⁶¹, S. Mergelmeyer¹⁷, P. Mermod⁵¹, L. Merola^{104a,104b}, C. Meroni^{92a}, F.S. Merritt³³, A. Messina^{132a,132b}, J. Metcalfe⁶, A.S. Mete¹⁶², C. Meyer⁸⁴, C. Meyer¹²², J.-P. Meyer¹³⁶, J. Meyer¹⁰⁷, H. Meyer Zu Theenhausen^{59a}, F. Miano¹⁴⁹, R.P. Middleton¹³¹, S. Miglioranza^{52a,52b}, L. Mijović²³, G. Mikenberg¹⁷¹, M. Mikestikova¹²⁷, M. Mikuz⁷⁶, M. Milesi⁸⁹, A. Milic⁶³, D.W. Miller³³, C. Mills⁴⁸, A. Milov¹⁷¹, D.A. Milstead^{146a,146b}, A.A. Minaenko¹³⁰, Y. Minami¹⁵⁵, I.A. Minashvili⁶⁶, A.I. Mincer¹¹⁰, B. Mindur^{40a}, M. Mineev⁶⁶, Y. Ming¹⁷², L.M. Mir¹³, K.P. Mistry¹²², T. Mitani¹⁷⁰, J. Mitrevski¹⁰⁰, V.A. Mitsou¹⁶⁶, A. Miucci⁵¹, P.S. Miyagawa¹³⁹, J.U. Mjörnmark⁸², T. Moa^{146a,146b}, K. Mochizuki⁹⁵, S. Mohapatra³⁷, S. Molander^{146a,146b}, R. Moles-Valls²³, R. Monden⁶⁹, M.C. Mondragon⁹¹, K. Mönig⁴⁴, J. Monk³⁸, E. Monnier⁸⁶, A. Montalbano¹⁴⁸, J. Montejo Berlingen³², F. Monticelli⁷², S. Monzani^{92a,92b},

R.W. Moore³, N. Morange¹¹⁷, D. Moreno²¹, M. Moreno Ll  cer⁵⁶, P. Morettini^{52a}, D. Mori¹⁴², T. Mori¹⁵⁵, M. Morii⁵⁸, M. Morinaga¹⁵⁵, V. Morisbak¹¹⁹, S. Moritz⁸⁴, A.K. Morley¹⁵⁰, G. Mornacchi³², J.D. Morris⁷⁷, S.S. Mortensen³⁸, L. Morvaj¹⁴⁸, M. Mosidze^{53b}, J. Moss¹⁴³, K. Motohashi¹⁵⁷, R. Mount¹⁴³, E. Mountricha²⁷, S.V. Mouraviev^{96,*}, E.J.W. Moyse⁸⁷, S. Muanza⁸⁶, R.D. Mudd¹⁹, F. Mueller¹⁰¹, J. Mueller¹²⁵, R.S.P. Mueller¹⁰⁰, T. Mueller³⁰, D. Muenstermann⁷³, P. Mullen⁵⁵, G.A. Mullier¹⁸, F.J. Munoz Sanchez⁸⁵, J.A. Murillo Quijada¹⁹, W.J. Murray^{169,131}, H. Musheghyan⁵⁶, M. Mu  skinja⁷⁶, A.G. Myagkov^{130,ae}, M. Myska¹²⁸, B.P. Nachman¹⁴³, O. Nackenhorst⁵¹, K. Nagai¹²⁰, R. Nagai^{67,2}, K. Nagano⁶⁷, Y. Nagasaka⁶⁰, K. Nagata¹⁶⁰, M. Nagel⁵⁰, E. Nagy⁸⁶, A.M. Nairz³², Y. Nakahama³², K. Nakamura⁶⁷, T. Nakamura¹⁵⁵, I. Nakano¹¹², H. Namasivayam⁴³, R.F. Naranjo Garcia⁴⁴, R. Narayan¹¹, D.I. Narrias Villar^{59a}, I. Naryshkin¹²³, T. Naumann⁴⁴, G. Navarro²¹, R. Nayyar⁷, H.A. Neal⁹⁰, P.Yu. Nechaeva⁹⁶, T.J. Neep⁸⁵, P.D. Nef¹⁴³, A. Negri^{121a,121b}, M. Negrini^{22a}, S. Nektarijevic¹⁰⁶, C. Nellist¹¹⁷, A. Nelson¹⁶², S. Nemecek¹²⁷, P. Nemethy¹¹⁰, A.A. Nepomuceno^{26a}, M. Nessi^{32,qf}, M.S. Neubauer¹⁶⁵, M. Neumann¹⁷⁴, R.M. Neves¹¹⁰, P. Nevski²⁷, P.R. Newman¹⁹, D.H. Nguyen⁶, T. Nguyen Manh⁹⁵, R.B. Nickerson¹²⁰, R. Nicolaidou¹³⁶, J. Nielsen¹³⁷, A. Nikiforov¹⁷, V. Nikolaenko^{130,ae}, I. Nikolic-Audit⁸¹, K. Nikolopoulos¹⁹, J.K. Nilsen¹¹⁹, P. Nilsson²⁷, Y. Ninomiya¹⁵⁵, A. Nisati^{132a}, R. Nisius¹⁰¹, T. Nobe¹⁵⁵, M. Nomachi¹¹⁸, I. Nomidis³¹, T. Nooney⁷⁷, S. Norberg¹¹³, M. Nordberg³², N. Norjoharuddeen¹²⁰, O. Novgorodova⁴⁶, S. Nowak¹⁰¹, M. Nozaki⁶⁷, L. Nozka¹¹⁵, K. Ntekas¹⁰, E. Nurse⁷⁹, F. Nuti⁸⁹, F. O'grady⁷, D.C. O'Neil¹⁴², A.A. O'Rourke⁴⁴, V. O'Shea⁵⁵, F.G. Oakham^{31,d}, H. Oberlack¹⁰¹, T. Obermann²³, J. Ocariz⁸¹, A. Ochi⁶⁸, I. Ochoa³⁷, J.P. Ochoa-Ricoux^{34a}, S. Oda⁷¹, S. Odaka⁶⁷, H. Ogren⁶², A. Oh⁸⁵, S.H. Oh⁴⁷, C.C. Ohm¹⁶, H. Ohman¹⁶⁴, H. Oide³², H. Okawa¹⁶⁰, Y. Okumura³³, T. Okuyama⁶⁷, A. Olariu^{28b}, L.F. Oleiro Seabra^{126a}, S.A. Olivares Pino⁴⁸, D. Oliveira Damazio²⁷, A. Olszewski⁴¹, J. Olszowska⁴¹, A. Onofre^{126a,126e}, K. Onogi¹⁰³, P.U.E. Onyisi^{11,v}, M.J. Oreglia³³, Y. Oren¹⁵³, D. Orestano^{134a,134b}, N. Orlando^{61b}, R.S. Orr¹⁵⁸, B. Osculati^{52a,52b}, R. Ospanov⁸⁵, G. Otero y Garzon²⁹, H. Otono⁷¹, M. Ouchrif^{135d}, F. Ould-Saada¹¹⁹, A. Ouraou¹³⁶, K.P. Oussoren¹⁰⁷, Q. Ouyang^{35a}, M. Owen⁵⁵, R.E. Owen¹⁹, V.E. Ozcan^{20a}, N. Ozturk⁸, K. Pachal¹⁴², A. Pacheco Pages¹³, L. Pacheco Rodriguez¹³⁶, C. Padilla Aranda¹³, M. Pa    ov  ⁵⁰, S. Pagan Griso¹⁶, F. Paige²⁷, P. Pais⁸⁷, K. Pajchel¹¹⁹, G. Palacino^{159b}, S. Palestini³², M. Palka^{40b}, D. Pallin³⁶, A. Palma^{126a,126b}, E. St. Panagiotopoulou¹⁰, C.E. Pandini⁸¹, J.G. Panduro Vazquez⁷⁸, P. Pani^{146a,146b}, S. Panitkin²⁷, D. Pantea^{28b}, L. Paolozzi⁵¹, Th.D. Papadopoulou¹⁰, K. Papageorgiou¹⁵⁴, A. Paramonov⁶, D. Paredes Hernandez¹⁷⁵, A.J. Parker⁷³, M.A. Parker³⁰, K.A. Parker¹³⁹, F. Parodi^{52a,52b}, J.A. Parsons³⁷, U. Parzefall⁵⁰, V.R. Pascuzzi¹⁵⁸, E. Pasqualucci^{132a}, S. Passaggio^{52a}, Fr. Pastore⁷⁸, G. P  sztor^{31,ag}, S. Pataria¹⁷⁴, J.R. Pater⁸⁵, T. Pauly³², J. Pearce¹⁶⁸, B. Pearson¹¹³, L.E. Pedersen³⁸, M. Pedersen¹¹⁹, S. Pedraza Lopez¹⁶⁶, R. Pedro^{126a,126b}, S.V. Peleganchuk^{109,c}, D. Pelikan¹⁶⁴, O. Penc¹²⁷, C. Peng^{35a}, H. Peng^{35b}, J. Penwell⁶², B.S. Peralva^{26b}, M.M. Perego¹³⁶, D.V. Perepelitsa²⁷, E. Perez Codina^{159a}, L. Perini^{92a,92b}, H. Pernegger³², S. Perrella^{104a,104b}, R. Peschke⁴⁴, V.D. Peshekhonov⁶⁶, K. Peters⁴⁴, R.F.Y. Peters⁸⁵, B.A. Petersen³², T.C. Petersen³⁸, E. Petit⁵⁷, A. Petridis¹, C. Petridou¹⁵⁴, P. Petroff¹¹⁷, E. Petrolo^{132a}, M. Petrov¹²⁰, F. Petrucci^{134a,134b}, N.E. Pettersson⁸⁷, A. Peyaud¹³⁶, R. Pezoa^{34b}, P.W. Phillips¹³¹, G. Piacquadio¹⁴³, E. Pianori¹⁶⁹, A. Picazio⁸⁷, E. Piccaro⁷⁷, M. Piccinini^{22a,22b}, M.A. Pickering¹²⁰, R. Piegaia²⁹, J.E. Pilcher³³, A.D. Pilkington⁸⁵, A.W.J. Pin⁸⁵, M. Pinamonti^{163a,163c,ah}, J.L. Pinfold³, A. Pingel³⁸, S. Pires⁸¹, H. Pirumov⁴⁴, M. Pitt¹⁷¹, L. Plazak^{144a}, M.-A. Pleier²⁷, V. Pleskot⁸⁴, E. Plotnikova⁶⁶, P. Plucinski⁹¹, D. Pluth⁶⁵, R. Poettgen^{146a,146b}, L. Poggioli¹¹⁷, D. Pohl²³, G. Polesello^{121a}, A. Poley⁴⁴, A. Policicchio^{39a,39b}, R. Polifka¹⁵⁸, A. Polini^{22a}, C.S. Pollard⁵⁵, V. Polychronakos²⁷, K. Pomm  s³², L. Pontecorvo^{132a}, B.G. Pope⁹¹, G.A. Popeneciu^{28c}, D.S. Popovic¹⁴, A. Poppleton³², S. Pospisil¹²⁸, K. Potamianos¹⁶, I.N. Potrap⁶⁶, C.J. Potter³⁰, C.T. Potter¹¹⁶, G. Poulard³², J. Poveda³², V. Pozdnyakov⁶⁶, M.E. Pozo Astigarraga³², P. Pralavorio⁸⁶, A. Pranko¹⁶, S. Prell⁶⁵, D. Price⁸⁵, L.E. Price⁶, M. Primavera^{74a}, S. Prince⁸⁸, K. Prokofiev^{61c}, F. Prokoshin^{34b}, S. Protopopescu²⁷, J. Proudfoot⁶, M. Przybycien^{40a}, D. Puddu^{134a,134b}, M. Purohit^{27,ai}, P. Puzo¹¹⁷, J. Qian⁹⁰, G. Qin⁵⁵, Y. Qin⁸⁵, A. Quadt⁵⁶, W.B. Quayle^{163a,163b}, M. Queitsch-Maitland⁸⁵, D. Quilty⁵⁵, S. Raddum¹¹⁹, V. Radeka²⁷, V. Radescu^{59b}, S.K. Radhakrishnan¹⁴⁸, P. Radloff¹¹⁶, P. Rados⁸⁹, F. Ragusa^{92a,92b}, G. Rahal¹⁷⁷, J.A. Raine⁸⁵, S. Rajagopalan²⁷, M. Rammensee³², C. Rangel-Smith¹⁶⁴, M.G. Ratti^{92a,92b}, F. Rauscher¹⁰⁰, S. Rave⁸⁴, T. Ravenscroft⁵⁵, I. Ravinovich¹⁷¹, M. Raymond³², A.L. Read¹¹⁹, N.P. Readoff⁷⁵, M. Reale^{74a,74b}, D.M. Rebuzzi^{121a,121b}, A. Redelbach¹⁷³, G. Redlinger²⁷, R. Reece¹³⁷,

K. Reeves⁴³, L. Rehnisch¹⁷, J. Reichert¹²², H. Reisin²⁹, C. Rembser³², H. Ren^{35a}, M. Rescigno^{132a}, S. Resconi^{92a}, E.D. Resseguie¹²², O.L. Rezanova^{109,c}, P. Reznicek¹²⁹, R. Rezvani⁹⁵, R. Richter¹⁰¹, S. Richter⁷⁹, E. Richter-Was^{40b}, O. Ricken²³, M. Ridel⁸¹, P. Rieck¹⁷, C.J. Riegel¹⁷⁴, J. Rieger⁵⁶, O. Rifki¹¹³, M. Rijssenbeek¹⁴⁸, A. Rimoldi^{121a,121b}, M. Rimoldi¹⁸, L. Rinaldi^{22a}, B. Ristić⁵¹, E. Ritsch³², I. Riu¹³, F. Rizatdinova¹¹⁴, E. Rizvi⁷⁷, C. Rizzi¹³, S.H. Robertson^{88,l}, A. Robichaud-Veronneau⁸⁸, D. Robinson³⁰, J.E.M. Robinson⁴⁴, A. Robson⁵⁵, C. Roda^{124a,124b}, Y. Rodina⁸⁶, A. Rodriguez Perez¹³, D. Rodriguez Rodriguez¹⁶⁶, S. Roe³², C.S. Rogan⁵⁸, O. Røhne¹¹⁹, A. Romanouk⁹⁸, M. Romano^{22a,22b}, S.M. Romano Saez³⁶, E. Romero Adam¹⁶⁶, N. Rompotis¹³⁸, M. Ronzani⁵⁰, L. Roos⁸¹, E. Ros¹⁶⁶, S. Rosati^{132a}, K. Rosbach⁵⁰, P. Rose¹³⁷, O. Rosenthal¹⁴¹, N.-A. Rosien⁵⁶, V. Rossetti^{146a,146b}, E. Rossi^{104a,104b}, L.P. Rossi^{52a}, J.H.N. Rosten³⁰, R. Rosten¹³⁸, M. Rotaru^{28b}, I. Roth¹⁷¹, J. Rothberg¹³⁸, D. Rousseau¹¹⁷, C.R. Royon¹³⁶, A. Rozanov⁸⁶, Y. Rozen¹⁵², X. Ruan^{145c}, F. Rubbo¹⁴³, M.S. Rudolph¹⁵⁸, F. Rühr⁵⁰, A. Ruiz-Martinez³¹, Z. Rurikova⁵⁰, N.A. Rusakovich⁶⁶, A. Ruschke¹⁰⁰, H.L. Russell¹³⁸, J.P. Rutherford⁷, N. Ruthmann³², Y.F. Ryabov¹²³, M. Rybar¹⁶⁵, G. Rybkin¹¹⁷, S. Ryu⁶, A. Ryzhov¹³⁰, G.F. Rzehorz⁵⁶, A.F. Saavedra¹⁵⁰, G. Sabato¹⁰⁷, S. Sacerdoti²⁹, H.F.-W. Sadrozinski¹³⁷, R. Sadykov⁶⁶, F. Safai Tehrani^{132a}, P. Saha¹⁰⁸, M. Sahinsoy^{59a}, M. Saimpert¹³⁶, T. Saito¹⁵⁵, H. Sakamoto¹⁵⁵, Y. Sakurai¹⁷⁰, G. Salamanna^{134a,134b}, A. Salamon^{133a,133b}, J.E. Salazar Loyola^{34b}, D. Salek¹⁰⁷, P.H. Sales De Bruin¹³⁸, D. Salihagic¹⁰¹, A. Salnikov¹⁴³, J. Salt¹⁶⁶, D. Salvatore^{39a,39b}, F. Salvatore¹⁴⁹, A. Salvucci^{61a}, A. Salzburger³², D. Sammel⁵⁰, D. Sampsonidis¹⁵⁴, A. Sanchez^{104a,104b}, J. Sánchez¹⁶⁶, V. Sanchez Martinez¹⁶⁶, H. Sandaker¹¹⁹, R.L. Sandbach⁷⁷, H.G. Sander⁸⁴, M. Sandhoff¹⁷⁴, C. Sandoval²¹, R. Sandstroem¹⁰¹, D.P.C. Sankey¹³¹, M. Sannino^{52a,52b}, A. Sansoni⁴⁹, C. Santoni³⁶, R. Santonico^{133a,133b}, H. Santos^{126a}, I. Santoyo Castillo¹⁴⁹, K. Sapp¹²⁵, A. Sapronov⁶⁶, J.G. Saraiva^{126a,126d}, B. Sarrazin²³, O. Sasaki⁶⁷, Y. Sasaki¹⁵⁵, K. Sato¹⁶⁰, G. Sauvage^{5,*}, E. Sauvan⁵, G. Savage⁷⁸, P. Savard^{158,d}, C. Sawyer¹³¹, L. Sawyer^{80,q}, J. Saxon³³, C. Sbarra^{22a}, A. Sbrizzi^{22a,22b}, T. Scanlon⁷⁹, D.A. Scannicchio¹⁶², M. Scarcella¹⁵⁰, V. Scarfone^{39a,39b}, J. Schaarschmidt¹⁷¹, P. Schacht¹⁰¹, B.M. Schachtner¹⁰⁰, D. Schaefer³², R. Schaefer⁴⁴, J. Schaeffer⁸⁴, S. Schaepe²³, S. Schaetzel^{59b}, U. Schäfer⁸⁴, A.C. Schaffer¹¹⁷, D. Schaile¹⁰⁰, R.D. Schamberger¹⁴⁸, V. Scharf^{59a}, V.A. Schegelsky¹²³, D. Scheirich¹²⁹, M. Schernau¹⁶², C. Schiavi^{52a,52b}, S. Schier¹³⁷, C. Schillo⁵⁰, M. Schioppa^{39a,39b}, S. Schlenker³², K.R. Schmidt-Sommerfeld¹⁰¹, K. Schmieden³², C. Schmitt⁸⁴, S. Schmitt⁴⁴, S. Schmitz⁸⁴, B. Schneider^{159a}, U. Schnoor⁵⁰, L. Schoeffel¹³⁶, A. Schoening^{59b}, B.D. Schoenrock⁹¹, E. Schopf²³, M. Schott⁸⁴, J. Schovancova⁸, S. Schramm⁵¹, M. Schreyer¹⁷³, N. Schuh⁸⁴, A. Schulte⁸⁴, M.J. Schultens²³, H.-C. Schultz-Coulon^{59a}, H. Schulz¹⁷, M. Schumacher⁵⁰, B.A. Schumm¹³⁷, Ph. Schune¹³⁶, A. Schwartzman¹⁴³, T.A. Schwarz⁹⁰, Ph. Schwegler¹⁰¹, H. Schweiger⁸⁵, Ph. Schwemling¹³⁶, R. Schwienhorst⁹¹, J. Schwindling¹³⁶, T. Schwindt²³, G. Sciolla²⁵, F. Scuri^{124a,124b}, F. Scutti⁸⁹, J. Searcy⁹⁰, P. Seema²³, S.C. Seidel¹⁰⁵, A. Seiden¹³⁷, F. Seifert¹²⁸, J.M. Seixas^{26a}, G. Sekhniaidze^{104a}, K. Sekhon⁹⁰, S.J. Sekula⁴², D.M. Seliverstov^{123,*}, N. Semprini-Cesari^{22a,22b}, C. Serfon¹¹⁹, L. Serin¹¹⁷, L. Serkin^{163a,163b}, M. Sessa^{134a,134b}, R. Seuster¹⁶⁸, H. Severini¹¹³, T. Sfiligoi⁷⁶, F. Sforza³², A. Sfyrla⁵¹, E. Shabalina⁵⁶, N.W. Shaikh^{146a,146b}, L.Y. Shan^{35a}, R. Shang¹⁶⁵, J.T. Shank²⁴, M. Shapiro¹⁶, P.B. Shatalov⁹⁷, K. Shaw^{163a,163b}, S.M. Shaw⁸⁵, A. Shcherbakova^{146a,146b}, C.Y. Shehu¹⁴⁹, P. Sherwood⁷⁹, L. Shi^{151,qj}, S. Shimizu⁶⁸, C.O. Shimmin¹⁶², M. Shimojima¹⁰², M. Shiyakova^{66,ak}, A. Shmeleva⁹⁶, D. Shoaleh Saadi⁹⁵, M.J. Shochet³³, S. Shojaii^{92a,92b}, S. Shrestha¹¹¹, E. Shulga⁹⁸, M.A. Shupe⁷, P. Sicho¹²⁷, A.M. Sickles¹⁶⁵, P.E. Sidebo¹⁴⁷, O. Sidiropoulou¹⁷³, D. Sidorov¹¹⁴, A. Sidoti^{22a,22b}, F. Siegert⁴⁶, Dj. Sijacki¹⁴, J. Silva^{126a,126d}, S.B. Silverstein^{146a}, V. Simak¹²⁸, O. Simard⁵, Lj. Simic¹⁴, S. Simion¹¹⁷, E. Simioni⁸⁴, B. Simmons⁷⁹, D. Simon³⁶, M. Simon⁸⁴, P. Sinervo¹⁵⁸, N.B. Sinev¹¹⁶, M. Sioli^{22a,22b}, G. Siragusa¹⁷³, S.Yu. Sivoklov⁹⁹, J. Sjölin^{146a,146b}, M.B. Skinner⁷³, H.P. Skottowe⁵⁸, P. Skubic¹¹³, M. Slater¹⁹, T. Slavicek¹²⁸, M. Slawinska¹⁰⁷, K. Sliwa¹⁶¹, R. Slovak¹²⁹, V. Smakhtin¹⁷¹, B.H. Smart⁵, L. Smestad¹⁵, J. Smiesko^{144a}, S.Yu. Smirnov⁹⁸, Y. Smirnov⁹⁸, L.N. Smirnova^{99,al}, O. Smirnova⁸², M.N.K. Smith³⁷, R.W. Smith³⁷, M. Smizanska⁷³, K. Smolek¹²⁸, A.A. Snesarev⁹⁶, S. Snyder²⁷, R. Sobie^{168,l}, F. Socher⁴⁶, A. Soffer¹⁵³, D.A. Soh¹⁵¹, G. Sokhrannyi⁷⁶, C.A. Solans Sanchez³², M. Solar¹²⁸, E.Yu. Soldatov⁹⁸, U. Soldevila¹⁶⁶, A.A. Solodkov¹³⁰, A. Soloshenko⁶⁶, O.V. Solovyanov¹³⁰, V. Solovyev¹²³, P. Sommer⁵⁰, H. Son¹⁶¹, H.Y. Song^{35b,am}, A. Sood¹⁶, A. Sopczak¹²⁸, V. Sopko¹²⁸, V. Sorin¹³, D. Sosa^{59b}, C.L. Sotiropoulou^{124a,124b}, R. Soualah^{163a,163c}, A.M. Soukharev^{109,c}, D. South⁴⁴, B.C. Sowden⁷⁸, S. Spagnolo^{74a,74b}, M. Spalla^{124a,124b}, M. Spangenberg¹⁶⁹, F. Spanò⁷⁸, D. Sperlich¹⁷,

F. Spettel¹⁰¹, R. Spighi^{22a}, G. Spigo³², L.A. Spiller⁸⁹, M. Spousta¹²⁹, R.D. St. Denis^{55,*}, A. Stabile^{92a}, R. Stamen^{59a}, S. Stamm¹⁷, E. Stanecka⁴¹, R.W. Stanek⁶, C. Stancu^{134a}, M. Stancu-Bellu⁴⁴, M.M. Stanitzki⁴⁴, S. Stapnes¹¹⁹, E.A. Starchenko¹³⁰, G.H. Stark³³, J. Stark⁵⁷, P. Staroba¹²⁷, P. Starovoitov^{59a}, S. Stärz³², R. Staszewski⁴¹, P. Steinberg²⁷, B. Stelzer¹⁴², H.J. Stelzer³², O. Stelzer-Chilton^{159a}, H. Stenzel⁵⁴, G.A. Stewart⁵⁵, J.A. Stillings²³, M.C. Stockton⁸⁸, M. Stoebe⁸⁸, G. Stoicea^{28b}, P. Stolte⁵⁶, S. Stonjek¹⁰¹, A.R. Stradling⁸, A. Straessner⁴⁶, M.E. Stramaglia¹⁸, J. Strandberg¹⁴⁷, S. Strandberg^{146a,146b}, A. Strandlie¹¹⁹, M. Strauss¹¹³, P. Strizenec^{144b}, R. Ströhmer¹⁷³, D.M. Strom¹¹⁶, R. Stroynowski⁴², A. Strubig¹⁰⁶, S.A. Stucci¹⁸, B. Stugu¹⁵, N.A. Styles⁴⁴, D. Su¹⁴³, J. Su¹²⁵, S. Suchek^{59a}, Y. Sugaya¹¹⁸, M. Suk¹²⁸, V.V. Sulin⁹⁶, S. Sultansoy^{4c}, T. Sumida⁶⁹, S. Sun⁵⁸, X. Sun^{35a}, J.E. Sundermann⁵⁰, K. Suruliz¹⁴⁹, G. Susinno^{39a,39b}, M.R. Sutton¹⁴⁹, S. Suzuki⁶⁷, M. Svatos¹²⁷, M. Swiatlowski³³, I. Sykora^{144a}, T. Sykora¹²⁹, D. Ta⁵⁰, C. Taccini^{134a,134b}, K. Tackmann⁴⁴, J. Taenzer¹⁵⁸, A. Taffard¹⁶², R. Tafiout^{159a}, N. Taiblum¹⁵³, H. Takai²⁷, R. Takashima⁷⁰, T. Takeshita¹⁴⁰, Y. Takubo⁶⁷, M. Talby⁸⁶, A.A. Talyshv^{109,c}, K.G. Tan⁸⁹, J. Tanaka¹⁵⁵, R. Tanaka¹¹⁷, S. Tanaka⁶⁷, B.B. Tannenwald¹¹¹, S. Tapia Araya^{34b}, S. Tapprogge⁸⁴, S. Tarem¹⁵², G.F. Tartarelli^{92a}, P. Tas¹²⁹, M. Tasevsky¹²⁷, T. Tashiro⁶⁹, E. Tassi^{39a,39b}, A. Tavares Delgado^{126a,126b}, Y. Tayalati^{135e}, A.C. Taylor¹⁰⁵, G.N. Taylor⁸⁹, P.T.E. Taylor⁸⁹, W. Taylor^{159b}, F.A. Teischinger³², P. Teixeira-Dias⁷⁸, K.K. Temming⁵⁰, D. Temple¹⁴², H. Ten Kate³², P.K. Teng¹⁵¹, J.J. Teoh¹¹⁸, F. Tepel¹⁷⁴, S. Terada⁶⁷, K. Terashi¹⁵⁵, J. Terron⁸³, S. Terzo¹⁰¹, M. Testa⁴⁹, R.J. Teuscher^{158,l}, T. Theveneaux-Pelzer⁸⁶, J.P. Thomas¹⁹, J. Thomas-Wilsker⁷⁸, E.N. Thompson³⁷, P.D. Thompson¹⁹, A.S. Thompson⁵⁵, L.A. Thomsen¹⁷⁵, E. Thomson¹²², M. Thomson³⁰, M.J. Tibbetts¹⁶, R.E. Ticse Torres⁸⁶, V.O. Tikhomirov^{96,an}, Yu.A. Tikhonov^{109,c}, S. Timoshenko⁹⁸, P. Tipton¹⁷⁵, S. Tisserant⁸⁶, K. Todome¹⁵⁷, T. Todorov^{5,*}, S. Todorova-Nova¹²⁹, J. Tojo⁷¹, S. Tokár^{144a}, K. Tokushuku⁶⁷, E. Tolley⁵⁸, L. Tomlinson⁸⁵, M. Tomoto¹⁰³, L. Tompkins^{143,ao}, K. Toms¹⁰⁵, B. Tong⁵⁸, E. Torrence¹¹⁶, H. Torres¹⁴², E. Torró Pastor¹³⁸, J. Toth^{86,ap}, F. Touchard⁸⁶, D.R. Tovey¹³⁹, T. Trefzger¹⁷³, A. Tricoli²⁷, I.M. Trigger^{159a}, S. Trincaz-Duvoid⁸¹, M.F. Tripiana¹³, W. Trischuk¹⁵⁸, B. Trocmé⁵⁷, A. Trofymov⁴⁴, C. Troncon^{92a}, M. Trotter-McDonald¹⁶, M. Trovatelli¹⁶⁸, L. Truong^{163a,163c}, M. Trzebinski⁴¹, A. Trzupek⁴¹, J.C.-L. Tseng¹²⁰, P.V. Tsiareshka⁹³, G. Tsipolitis¹⁰, N. Tsirintanis⁹, S. Tsiskaridze¹³, V. Tsiskaridze⁵⁰, E.G. Tskhadadze^{53a}, K.M. Tsui^{61a}, I.I. Tsukerman⁹⁷, V. Tsulaia¹⁶, S. Tsuno⁶⁷, D. Tsybychev¹⁴⁸, A. Tudorache^{28b}, V. Tudorache^{28b}, A.N. Tuna⁵⁸, S.A. Tupputi^{22a,22b}, S. Turchikhin^{99,al}, D. Turecek¹²⁸, D. Turgeman¹⁷¹, R. Turra^{92a,92b}, A.J. Turvey⁴², P.M. Tuts³⁷, M. Tyndel¹³¹, G. Uccielli^{22a,22b}, I. Ueda¹⁵⁵, M. Ughetto^{146a,146b}, F. Ukegawa¹⁶⁰, G. Unal³², A. Undrus²⁷, G. Unel¹⁶², F.C. Ungaro⁸⁹, Y. Unno⁶⁷, C. Unverdorben¹⁰⁰, J. Urban^{144b}, P. Urquijo⁸⁹, P. Urrejola⁸⁴, G. Usai⁸, A. Usanova⁶³, L. Vacavant⁸⁶, V. Vacek¹²⁸, B. Vachon⁸⁸, C. Valderanis¹⁰⁰, E. Valdes Santurio^{146a,146b}, N. Valencic¹⁰⁷, S. Valentineti^{22a,22b}, A. Valero¹⁶⁶, L. Valery¹³, S. Valkar¹²⁹, S. Vallecorsa⁵¹, J.A. Valls Ferrer¹⁶⁶, W. Van Den Wollenberg¹⁰⁷, P.C. Van Der Deijl¹⁰⁷, R. van der Geer¹⁰⁷, H. van der Graaf¹⁰⁷, N. van Eldik¹⁵², P. van Gemmeren⁶, J. Van Nieuwkoop¹⁴², I. van Vulpen¹⁰⁷, M.C. van Woerden³², M. Vanadia^{132a,132b}, W. Vandelli³², R. Vanguri¹²², A. Vaniachine¹³⁰, P. Vankov¹⁰⁷, G. Vardanyan¹⁷⁶, R. Vari^{132a}, E.W. Varnes⁷, T. Varol⁴², D. Varouchas⁸¹, A. Vartapetian⁸, K.E. Varvell¹⁵⁰, J.G. Vasquez¹⁷⁵, F. Vazeille³⁶, T. Vazquez Schroeder⁸⁸, J. Veatch⁵⁶, L.M. Veloce¹⁵⁸, F. Veloso^{126a,126c}, S. Veneziano^{132a}, A. Ventura^{74a,74b}, M. Venturi¹⁶⁸, N. Venturi¹⁵⁸, A. Venturini²⁵, V. Vercesi^{121a}, M. Verducci^{132a,132b}, W. Verkerke¹⁰⁷, J.C. Vermeulen¹⁰⁷, A. Vest^{46,aq}, M.C. Vetterli^{142,d}, O. Viazlo⁸², I. Vichou^{165,*}, T. Vickey¹³⁹, O.E. Vickey Boeriu¹³⁹, G.H.A. Viehhauser¹²⁰, S. Viel¹⁶, L. Vigani¹²⁰, M. Villa^{22a,22b}, M. Villaplana Perez^{92a,92b}, E. Vilucchi⁴⁹, M.G. Vinciter³¹, V.B. Vinogradov⁶⁶, C. Vittori^{22a,22b}, I. Vivarelli¹⁴⁹, S. Vlachos¹⁰, M. Vlasak¹²⁸, M. Vogel¹⁷⁴, P. Vokac¹²⁸, G. Volpi^{124a,124b}, M. Volpi⁸⁹, H. von der Schmitt¹⁰¹, E. von Toerne²³, V. Vorobel¹²⁹, K. Vorobev⁹⁸, M. Vos¹⁶⁶, R. Voss³², J.H. Vossebeld⁷⁵, N. Vranjes¹⁴, M. Vranjes Milosavljevic¹⁴, V. Vrba¹²⁷, M. Vreeswijk¹⁰⁷, R. Vuillermet³², I. Vukotic³³, Z. Vykydal¹²⁸, P. Wagner²³, W. Wagner¹⁷⁴, H. Wahlberg⁷², S. Wahrmund⁴⁶, J. Wakabayashi¹⁰³, J. Walder⁷³, R. Walker¹⁰⁰, W. Walkowiak¹⁴¹, V. Wallangen^{146a,146b}, C. Wang^{35c}, C. Wang^{35d,86}, F. Wang¹⁷², H. Wang¹⁶, H. Wang⁴², J. Wang⁴⁴, J. Wang¹⁵⁰, K. Wang⁸⁸, R. Wang⁶, S.M. Wang¹⁵¹, T. Wang²³, T. Wang³⁷, W. Wang^{35b}, X. Wang¹⁷⁵, C. Wanotayaroj¹¹⁶, A. Warburton⁸⁸, C.P. Ward³⁰, D.R. Wardrope⁷⁹, A. Washbrook⁴⁸, P.M. Watkins¹⁹, A.T. Watson¹⁹, M.F. Watson¹⁹, G. Watts¹³⁸, S. Watts⁸⁵, B.M. Waugh⁷⁹, S. Webb⁸⁴, M.S. Weber¹⁸, S.W. Weber¹⁷³, J.S. Webster⁶, A.R. Weidberg¹²⁰, B. Weinert⁶², J. Weingarten⁵⁶, C. Weiser⁵⁰,

H. Weits¹⁰⁷, P.S. Wells³², T. Wenaus²⁷, T. Wengler³², S. Wenig³², N. Wermes²³, M. Werner⁵⁰, M.D. Werner⁶⁵, P. Werner³², M. Wessels^{59a}, J. Wetter¹⁶¹, K. Whalen¹¹⁶, N.L. Whallon¹³⁸, A.M. Wharton⁷³, A. White⁸, M.J. White¹, R. White^{34b}, D. Whiteson¹⁶², F.J. Wickens¹³¹, W. Wiedenmann¹⁷², M. Wielers¹³¹, P. Wienemann²³, C. Wiglesworth³⁸, L.A.M. Wiik-Fuchs²³, A. Wildauer¹⁰¹, F. Wilk⁸⁵, H.G. Wilkens³², H.H. Williams¹²², S. Williams¹⁰⁷, C. Willis⁹¹, S. Willocq⁸⁷, J.A. Wilson¹⁹, I. Wingerter-Seez⁵, F. Winklmeier¹¹⁶, O.J. Winston¹⁴⁹, B.T. Winter²³, M. Wittgen¹⁴³, J. Wittkowski¹⁰⁰, T.M.H. Wolf¹⁰⁷, M.W. Wolter⁴¹, H. Wolters^{126a,126c}, S.D. Worm¹³¹, B.K. Wosiek⁴¹, J. Wotschack³², M.J. Woudstra⁸⁵, K.W. Wozniak⁴¹, M. Wu⁵⁷, M. Wu³³, S.L. Wu¹⁷², X. Wu⁵¹, Y. Wu⁹⁰, T.R. Wyatt⁸⁵, B.M. Wynne⁴⁸, S. Xella³⁸, D. Xu^{35a}, L. Xu²⁷, B. Yabsley¹⁵⁰, S. Yacoob^{145a}, R. Yakabe⁶⁸, D. Yamaguchi¹⁵⁷, Y. Yamaguchi¹¹⁸, A. Yamamoto⁶⁷, S. Yamamoto¹⁵⁵, T. Yamanaka¹⁵⁵, K. Yamauchi¹⁰³, Y. Yamazaki⁶⁸, Z. Yan²⁴, H. Yang^{35e}, H. Yang¹⁷², Y. Yang¹⁵¹, Z. Yang¹⁵, W.-M. Yao¹⁶, Y.C. Yap⁸¹, Y. Yasu⁶⁷, E. Yatsenko⁵, K.H. Yau Wong²³, J. Ye⁴², S. Ye²⁷, I. Yeletsikh⁶⁶, A.L. Yen⁵⁸, E. Yildirim⁸⁴, K. Yorita¹⁷⁰, R. Yoshida⁶, K. Yoshihara¹²², C. Young¹⁴³, C.J.S. Young³², S. Youssef²⁴, D.R. Yu¹⁶, J. Yu⁸, J.M. Yu⁹⁰, J. Yu⁶⁵, L. Yuan⁶⁸, S.P.Y. Yuen²³, I. Yusuff^{30,ar}, B. Zabinski⁴¹, R. Zaidan^{35d}, A.M. Zaitsev^{130,ae}, N. Zakharchuk⁴⁴, J. Zalieckas¹⁵, A. Zaman¹⁴⁸, S. Zambito⁵⁸, L. Zanello^{132a,132b}, D. Zanzi⁸⁹, C. Zeitnitz¹⁷⁴, M. Zeman¹²⁸, A. Zemla^{40a}, J.C. Zeng¹⁶⁵, Q. Zeng¹⁴³, K. Zengel²⁵, O. Zenin¹³⁰, T. Ženiš^{144a}, D. Zerwas¹¹⁷, D. Zhang⁹⁰, F. Zhang¹⁷², G. Zhang^{35b,am}, H. Zhang^{35c}, J. Zhang⁶, L. Zhang⁵⁰, R. Zhang²³, R. Zhang^{35b,as}, X. Zhang^{35d}, Z. Zhang¹¹⁷, X. Zhao⁴², Y. Zhao^{35d}, Z. Zhao^{35b}, A. Zhemchugov⁶⁶, J. Zhong¹²⁰, B. Zhou⁹⁰, C. Zhou⁴⁷, L. Zhou³⁷, L. Zhou⁴², M. Zhou¹⁴⁸, N. Zhou^{35f}, C.G. Zhu^{35d}, H. Zhu^{35a}, J. Zhu⁹⁰, Y. Zhu^{35b}, X. Zhuang^{35a}, K. Zhukov⁹⁶, A. Zibell¹⁷³, D. Zieminska⁶², N.I. Zimine⁶⁶, C. Zimmermann⁸⁴, S. Zimmermann⁵⁰, Z. Zinonos⁵⁶, M. Zinser⁸⁴, M. Ziolkowski¹⁴¹, L. Živković¹⁴, G. Zobernig¹⁷², A. Zoccoli^{22a,22b}, M. zur Nedden¹⁷, L. Zwalinski³²

¹ Department of Physics, University of Adelaide, Adelaide, Australia

² Physics Department, SUNY Albany, Albany NY, United States

³ Department of Physics, University of Alberta, Edmonton AB, Canada

⁴ (a) Department of Physics, Ankara University, Ankara; (b) Istanbul Aydin University, Istanbul; (c) Division of Physics, TOBB University of Economics and Technology, Ankara, Turkey

⁵ LAPP, CNRS/IN2P3 and Université Savoie Mont Blanc, Annecy-le-Vieux, France

⁶ High Energy Physics Division, Argonne National Laboratory, Argonne IL, United States

⁷ Department of Physics, University of Arizona, Tucson AZ, United States

⁸ Department of Physics, The University of Texas at Arlington, Arlington TX, United States

⁹ Physics Department, University of Athens, Athens, Greece

¹⁰ Physics Department, National Technical University of Athens, Zografou, Greece

¹¹ Department of Physics, The University of Texas at Austin, Austin TX, United States

¹² Institute of Physics, Azerbaijan Academy of Sciences, Baku, Azerbaijan

¹³ Institut de Física d'Altes Energies (IFAE), The Barcelona Institute of Science and Technology, Barcelona, Spain

¹⁴ Institute of Physics, University of Belgrade, Belgrade, Serbia

¹⁵ Department for Physics and Technology, University of Bergen, Bergen, Norway

¹⁶ Physics Division, Lawrence Berkeley National Laboratory and University of California, Berkeley CA, United States

¹⁷ Department of Physics, Humboldt University, Berlin, Germany

¹⁸ Albert Einstein Center for Fundamental Physics and Laboratory for High Energy Physics, University of Bern, Bern, Switzerland

¹⁹ School of Physics and Astronomy, University of Birmingham, Birmingham, United Kingdom

²⁰ (a) Department of Physics, Bogazici University, Istanbul; (b) Department of Physics Engineering, Gaziantep University, Gaziantep; (c) Istanbul Bilgi University, Faculty of Engineering and Natural Sciences, Istanbul; (d) Bahcesehir University, Faculty of Engineering and Natural Sciences, Istanbul, Turkey

²¹ Centro de Investigaciones, Universidad Antonio Narino, Bogota, Colombia

²² (a) INFN Sezione di Bologna; (b) Dipartimento di Fisica e Astronomia, Università di Bologna, Bologna, Italy

²³ Physikalisches Institut, University of Bonn, Bonn, Germany

²⁴ Department of Physics, Boston University, Boston MA, United States

²⁵ Department of Physics, Brandeis University, Waltham MA, United States

²⁶ (a) Universidade Federal do Rio de Janeiro COPPE/EE/IF, Rio de Janeiro; (b) Electrical Circuits Department, Federal University of Juiz de Fora (UFJF), Juiz de Fora; (c) Federal University of Sao Joao del Rei (UFSJ), Sao Joao del Rei; (d) Instituto de Física, Universidade de Sao Paulo, Sao Paulo, Brazil

²⁷ Physics Department, Brookhaven National Laboratory, Upton NY, United States

²⁸ (a) Transilvania University of Brasov, Brasov; (b) National Institute of Physics and Nuclear Engineering, Bucharest; (c) National Institute for Research and Development of Isotopic and Molecular Technologies, Physics Department, Cluj Napoca; (d) University Politehnica Bucharest, Bucharest; (e) West University in Timisoara, Timisoara, Romania

²⁹ Departamento de Física, Universidad de Buenos Aires, Buenos Aires, Argentina

³⁰ Cavendish Laboratory, University of Cambridge, Cambridge, United Kingdom

³¹ Department of Physics, Carleton University, Ottawa ON, Canada

³² CERN, Geneva, Switzerland

³³ Enrico Fermi Institute, University of Chicago, Chicago IL, United States

³⁴ (a) Departamento de Física, Pontificia Universidad Católica de Chile, Santiago; (b) Departamento de Física, Universidad Técnica Federico Santa María, Valparaíso, Chile

³⁵ (a) Institute of High Energy Physics, Chinese Academy of Sciences, Beijing; (b) Department of Modern Physics, University of Science and Technology of China, Anhui; (c) Department of Physics, Nanjing University, Jiangsu; (d) School of Physics, Shandong University, Shandong; (e) Department of Physics and Astronomy, Shanghai Key Laboratory for Particle Physics and Cosmology, Shanghai Jiao Tong University, Shanghai; (f) Physics Department, Tsinghua University, Beijing 100084, China

³⁶ Laboratoire de Physique Corpusculaire, Clermont Université et CNRS/IN2P3, Clermont-Ferrand, France

³⁷ Nevis Laboratory, Columbia University, Irvington NY, United States

³⁸ Niels Bohr Institute, University of Copenhagen, Copenhagen, Denmark

³⁹ (a) INFN Gruppo Collegato di Cosenza, Laboratori Nazionali di Frascati; (b) Dipartimento di Fisica, Università della Calabria, Rende, Italy

- ⁴⁰ (a) AGH University of Science and Technology, Faculty of Physics and Applied Computer Science, Krakow; (b) Marian Smoluchowski Institute of Physics, Jagiellonian University, Krakow, Poland
- ⁴¹ Institute of Nuclear Physics Polish Academy of Sciences, Krakow, Poland
- ⁴² Physics Department, Southern Methodist University, Dallas TX, United States
- ⁴³ Physics Department, University of Texas at Dallas, Richardson TX, United States
- ⁴⁴ DESY, Hamburg and Zeuthen, Germany
- ⁴⁵ Institut für Experimentelle Physik IV, Technische Universität Dortmund, Dortmund, Germany
- ⁴⁶ Institut für Kern- und Teilchenphysik, Technische Universität Dresden, Dresden, Germany
- ⁴⁷ Department of Physics, Duke University, Durham NC, United States
- ⁴⁸ SUPA – School of Physics and Astronomy, University of Edinburgh, Edinburgh, United Kingdom
- ⁴⁹ INFN Laboratori Nazionali di Frascati, Frascati, Italy
- ⁵⁰ Fakultät für Mathematik und Physik, Albert-Ludwigs-Universität, Freiburg, Germany
- ⁵¹ Section de Physique, Université de Genève, Geneva, Switzerland
- ⁵² (a) INFN Sezione di Genova; (b) Dipartimento di Fisica, Università di Genova, Genova, Italy
- ⁵³ (a) E. Andronikashvili Institute of Physics, Iv. Javakishvili Tbilisi State University, Tbilisi; (b) High Energy Physics Institute, Tbilisi State University, Tbilisi, Georgia
- ⁵⁴ II Physikalisches Institut, Justus-Liebig-Universität Giessen, Giessen, Germany
- ⁵⁵ SUPA – School of Physics and Astronomy, University of Glasgow, Glasgow, United Kingdom
- ⁵⁶ II Physikalisches Institut, Georg-August-Universität, Göttingen, Germany
- ⁵⁷ Laboratoire de Physique Subatomique et de Cosmologie, Université Grenoble-Alpes, CNRS/IN2P3, Grenoble, France
- ⁵⁸ Laboratory for Particle Physics and Cosmology, Harvard University, Cambridge MA, United States
- ⁵⁹ (a) Kirchhoff-Institut für Physik, Ruprecht-Karls-Universität Heidelberg, Heidelberg; (b) Physikalisches Institut, Ruprecht-Karls-Universität Heidelberg, Heidelberg; (c) ZITI Institut für technische Informatik, Ruprecht-Karls-Universität Heidelberg, Mannheim, Germany
- ⁶⁰ Faculty of Applied Information Science, Hiroshima Institute of Technology, Hiroshima, Japan
- ⁶¹ (a) Department of Physics, The Chinese University of Hong Kong, Shatin, N.T., Hong Kong; (b) Department of Physics, The University of Hong Kong, Hong Kong; (c) Department of Physics, The Hong Kong University of Science and Technology, Clear Water Bay, Kowloon, Hong Kong, China
- ⁶² Department of Physics, Indiana University, Bloomington IN, United States
- ⁶³ Institut für Astro- und Teilchenphysik, Leopold-Franzens-Universität, Innsbruck, Austria
- ⁶⁴ University of Iowa, Iowa City IA, United States
- ⁶⁵ Department of Physics and Astronomy, Iowa State University, Ames IA, United States
- ⁶⁶ Joint Institute for Nuclear Research, JINR Dubna, Dubna, Russia
- ⁶⁷ KEK, High Energy Accelerator Research Organization, Tsukuba, Japan
- ⁶⁸ Graduate School of Science, Kobe University, Kobe, Japan
- ⁶⁹ Faculty of Science, Kyoto University, Kyoto, Japan
- ⁷⁰ Kyoto University of Education, Kyoto, Japan
- ⁷¹ Department of Physics, Kyushu University, Fukuoka, Japan
- ⁷² Instituto de Física La Plata, Universidad Nacional de La Plata and CONICET, La Plata, Argentina
- ⁷³ Physics Department, Lancaster University, Lancaster, United Kingdom
- ⁷⁴ (a) INFN Sezione di Lecce; (b) Dipartimento di Matematica e Fisica, Università del Salento, Lecce, Italy
- ⁷⁵ Oliver Lodge Laboratory, University of Liverpool, Liverpool, United Kingdom
- ⁷⁶ Department of Physics, Jožef Stefan Institute and University of Ljubljana, Ljubljana, Slovenia
- ⁷⁷ School of Physics and Astronomy, Queen Mary University of London, London, United Kingdom
- ⁷⁸ Department of Physics, Royal Holloway University of London, Surrey, United Kingdom
- ⁷⁹ Department of Physics and Astronomy, University College London, London, United Kingdom
- ⁸⁰ Louisiana Tech University, Ruston LA, United States
- ⁸¹ Laboratoire de Physique Nucléaire et de Hautes Energies, UPMC and Université Paris-Diderot and CNRS/IN2P3, Paris, France
- ⁸² Fysiska institutionen, Lunds universitet, Lund, Sweden
- ⁸³ Departamento de Física Teórica C-15, Universidad Autónoma de Madrid, Madrid, Spain
- ⁸⁴ Institut für Physik, Universität Mainz, Mainz, Germany
- ⁸⁵ School of Physics and Astronomy, University of Manchester, Manchester, United Kingdom
- ⁸⁶ CPPM, Aix-Marseille Université and CNRS/IN2P3, Marseille, France
- ⁸⁷ Department of Physics, University of Massachusetts, Amherst MA, United States
- ⁸⁸ Department of Physics, McGill University, Montreal QC, Canada
- ⁸⁹ School of Physics, University of Melbourne, Victoria, Australia
- ⁹⁰ Department of Physics, The University of Michigan, Ann Arbor MI, United States
- ⁹¹ Department of Physics and Astronomy, Michigan State University, East Lansing MI, United States
- ⁹² (a) INFN Sezione di Milano; (b) Dipartimento di Fisica, Università di Milano, Milano, Italy
- ⁹³ B.I. Stepanov Institute of Physics, National Academy of Sciences of Belarus, Minsk, Belarus
- ⁹⁴ National Scientific and Educational Centre for Particle and High Energy Physics, Minsk, Belarus
- ⁹⁵ Group of Particle Physics, University of Montreal, Montreal QC, Canada
- ⁹⁶ P.N. Lebedev Physical Institute of the Russian Academy of Sciences, Moscow, Russia
- ⁹⁷ Institute for Theoretical and Experimental Physics (ITEP), Moscow, Russia
- ⁹⁸ National Research Nuclear University MEPhI, Moscow, Russia
- ⁹⁹ D.V. Skobeltsyn Institute of Nuclear Physics, M.V. Lomonosov Moscow State University, Moscow, Russia
- ¹⁰⁰ Fakultät für Physik, Ludwig-Maximilians-Universität München, München, Germany
- ¹⁰¹ Max-Planck-Institut für Physik (Werner-Heisenberg-Institut), München, Germany
- ¹⁰² Nagasaki Institute of Applied Science, Nagasaki, Japan
- ¹⁰³ Graduate School of Science and Kobayashi-Maskawa Institute, Nagoya University, Nagoya, Japan
- ¹⁰⁴ (a) INFN Sezione di Napoli; (b) Dipartimento di Fisica, Università di Napoli, Napoli, Italy
- ¹⁰⁵ Department of Physics and Astronomy, University of New Mexico, Albuquerque NM, United States
- ¹⁰⁶ Institute for Mathematics, Astrophysics and Particle Physics, Radboud University Nijmegen/Nikhef, Nijmegen, Netherlands
- ¹⁰⁷ Nikhef National Institute for Subatomic Physics and University of Amsterdam, Amsterdam, Netherlands
- ¹⁰⁸ Department of Physics, Northern Illinois University, DeKalb IL, United States
- ¹⁰⁹ Budker Institute of Nuclear Physics, SB RAS, Novosibirsk, Russia
- ¹¹⁰ Department of Physics, New York University, New York NY, United States
- ¹¹¹ Ohio State University, Columbus OH, United States
- ¹¹² Faculty of Science, Okayama University, Okayama, Japan
- ¹¹³ Homer L. Dodge Department of Physics and Astronomy, University of Oklahoma, Norman OK, United States
- ¹¹⁴ Department of Physics, Oklahoma State University, Stillwater OK, United States
- ¹¹⁵ Palacký University, RCPTM, Olomouc, Czech Republic

- ¹¹⁶ Center for High Energy Physics, University of Oregon, Eugene OR, United States
¹¹⁷ LAL, Univ. Paris-Sud, CNRS/IN2P3, Université Paris-Saclay, Orsay, France
¹¹⁸ Graduate School of Science, Osaka University, Osaka, Japan
¹¹⁹ Department of Physics, University of Oslo, Oslo, Norway
¹²⁰ Department of Physics, Oxford University, Oxford, United Kingdom
¹²¹ ^(a) INFN Sezione di Pavia; ^(b) Dipartimento di Fisica, Università di Pavia, Pavia, Italy
¹²² Department of Physics, University of Pennsylvania, Philadelphia PA, United States
¹²³ National Research Centre "Kurchatov Institute" B.P. Konstantinov Petersburg Nuclear Physics Institute, St. Petersburg, Russia
¹²⁴ ^(a) INFN Sezione di Pisa; ^(b) Dipartimento di Fisica E. Fermi, Università di Pisa, Pisa, Italy
¹²⁵ Department of Physics and Astronomy, University of Pittsburgh, Pittsburgh PA, United States
¹²⁶ ^(a) Laboratório de Instrumentação e Física Experimental de Partículas – LIP, Lisboa; ^(b) Faculdade de Ciências, Universidade de Lisboa, Lisboa; ^(c) Department of Physics, University of Coimbra, Coimbra; ^(d) Centro de Física Nuclear da Universidade de Lisboa, Lisboa; ^(e) Departamento de Física, Universidade do Minho, Braga; ^(f) Departamento de Física Teórica y del Cosmos and CAFPE, Universidad de Granada, Granada (Spain); ^(g) Dep Física and CEFITEC de Faculdade de Ciências e Tecnologia, Universidade Nova de Lisboa, Caparica, Portugal
¹²⁷ Institute of Physics, Academy of Sciences of the Czech Republic, Praha, Czech Republic
¹²⁸ Czech Technical University in Prague, Praha, Czech Republic
¹²⁹ Faculty of Mathematics and Physics, Charles University in Prague, Praha, Czech Republic
¹³⁰ State Research Center Institute for High Energy Physics (Protvino), NRC KI, Russia
¹³¹ Particle Physics Department, Rutherford Appleton Laboratory, Didcot, United Kingdom
¹³² ^(a) INFN Sezione di Roma; ^(b) Dipartimento di Fisica, Sapienza Università di Roma, Roma, Italy
¹³³ ^(a) INFN Sezione di Roma Tor Vergata; ^(b) Dipartimento di Fisica, Università di Roma Tor Vergata, Roma, Italy
¹³⁴ ^(a) INFN Sezione di Roma Tre; ^(b) Dipartimento di Matematica e Fisica, Università Roma Tre, Roma, Italy
¹³⁵ ^(a) Faculté des Sciences Ain Chock, Réseau Universitaire de Physique des Hautes Energies – Université Hassan II, Casablanca; ^(b) Centre National de l'Energie des Sciences Techniques Nucleaires, Rabat; ^(c) Faculté des Sciences Semlalia, Université Cadi Ayyad, LPHEA-Marrakech; ^(d) Faculté des Sciences, Université Mohamed Premier and LPTPM, Oujda; ^(e) Faculté des sciences, Université Mohammed V, Rabat, Morocco
¹³⁶ DSM/IRFU (Institut de Recherches sur les Lois Fondamentales de l'Univers), CEA Saclay (Commissariat à l'Energie Atomique et aux Energies Alternatives), Gif-sur-Yvette, France
¹³⁷ Santa Cruz Institute for Particle Physics, University of California Santa Cruz, Santa Cruz CA, United States
¹³⁸ Department of Physics, University of Washington, Seattle WA, United States
¹³⁹ Department of Physics and Astronomy, University of Sheffield, Sheffield, United Kingdom
¹⁴⁰ Department of Physics, Shinshu University, Nagano, Japan
¹⁴¹ Fachbereich Physik, Universität Siegen, Siegen, Germany
¹⁴² Department of Physics, Simon Fraser University, Burnaby BC, Canada
¹⁴³ SLAC National Accelerator Laboratory, Stanford CA, United States
¹⁴⁴ ^(a) Faculty of Mathematics, Physics & Informatics, Comenius University, Bratislava; ^(b) Department of Subnuclear Physics, Institute of Experimental Physics of the Slovak Academy of Sciences, Kosice, Slovak Republic
¹⁴⁵ ^(a) Department of Physics, University of Cape Town, Cape Town; ^(b) Department of Physics, University of Johannesburg, Johannesburg; ^(c) School of Physics, University of the Witwatersrand, Johannesburg, South Africa
¹⁴⁶ ^(a) Department of Physics, Stockholm University; ^(b) The Oskar Klein Centre, Stockholm, Sweden
¹⁴⁷ Physics Department, Royal Institute of Technology, Stockholm, Sweden
¹⁴⁸ Departments of Physics & Astronomy and Chemistry, Stony Brook University, Stony Brook NY, United States
¹⁴⁹ Department of Physics and Astronomy, University of Sussex, Brighton, United Kingdom
¹⁵⁰ School of Physics, University of Sydney, Sydney, Australia
¹⁵¹ Institute of Physics, Academia Sinica, Taipei, Taiwan
¹⁵² Department of Physics, Technion: Israel Institute of Technology, Haifa, Israel
¹⁵³ Raymond and Beverly Sackler School of Physics and Astronomy, Tel Aviv University, Tel Aviv, Israel
¹⁵⁴ Department of Physics, Aristotle University of Thessaloniki, Thessaloniki, Greece
¹⁵⁵ International Center for Elementary Particle Physics and Department of Physics, The University of Tokyo, Tokyo, Japan
¹⁵⁶ Graduate School of Science and Technology, Tokyo Metropolitan University, Tokyo, Japan
¹⁵⁷ Department of Physics, Tokyo Institute of Technology, Tokyo, Japan
¹⁵⁸ Department of Physics, University of Toronto, Toronto ON, Canada
¹⁵⁹ ^(a) TRIUMF, Vancouver BC; ^(b) Department of Physics and Astronomy, York University, Toronto ON, Canada
¹⁶⁰ Faculty of Pure and Applied Sciences, and Center for Integrated Research in Fundamental Science and Engineering, University of Tsukuba, Tsukuba, Japan
¹⁶¹ Department of Physics and Astronomy, Tufts University, Medford MA, United States
¹⁶² Department of Physics and Astronomy, University of California Irvine, Irvine CA, United States
¹⁶³ ^(a) INFN Gruppo Collegato di Udine, Sezione di Trieste, Udine; ^(b) ICTP, Trieste; ^(c) Dipartimento di Chimica, Fisica e Ambiente, Università di Udine, Udine, Italy
¹⁶⁴ Department of Physics and Astronomy, University of Uppsala, Uppsala, Sweden
¹⁶⁵ Department of Physics, University of Illinois, Urbana IL, United States
¹⁶⁶ Instituto de Física Corpuscular (IFIC) and Departamento de Física Atomica, Molecular y Nuclear and Departamento de Ingeniería Electrónica and Instituto de Microelectrónica de Barcelona (IMB-CNM), University of Valencia and CSIC, Valencia, Spain
¹⁶⁷ Department of Physics, University of British Columbia, Vancouver BC, Canada
¹⁶⁸ Department of Physics and Astronomy, University of Victoria, Victoria BC, Canada
¹⁶⁹ Department of Physics, University of Warwick, Coventry, United Kingdom
¹⁷⁰ Waseda University, Tokyo, Japan
¹⁷¹ Department of Particle Physics, The Weizmann Institute of Science, Rehovot, Israel
¹⁷² Department of Physics, University of Wisconsin, Madison WI, United States
¹⁷³ Fakultät für Physik und Astronomie, Julius-Maximilians-Universität, Würzburg, Germany
¹⁷⁴ Fakultät für Mathematik und Naturwissenschaften, Fachgruppe Physik, Bergische Universität Wuppertal, Wuppertal, Germany
¹⁷⁵ Department of Physics, Yale University, New Haven CT, United States
¹⁷⁶ Yerevan Physics Institute, Yerevan, Armenia
¹⁷⁷ Centre de Calcul de l'Institut National de Physique Nucléaire et de Physique des Particules (IN2P3), Villeurbanne, France

^a Also at Department of Physics, King's College London, London, United Kingdom.

^b Also at Institute of Physics, Azerbaijan Academy of Sciences, Baku, Azerbaijan.

^c Also at Novosibirsk State University, Novosibirsk, Russia.

^d Also at TRIUMF, Vancouver BC, Canada.

^e Also at Department of Physics & Astronomy, University of Louisville, Louisville, KY, United States.

^f Also at Department of Physics, California State University, Fresno CA, United States.

^g Also at Department of Physics, University of Fribourg, Fribourg, Switzerland.

^h Also at Departament de Física de la Universitat Autònoma de Barcelona, Barcelona, Spain.

- ⁱ Also at Departamento de Física e Astronomia, Faculdade de Ciências, Universidade do Porto, Portugal.
- ^j Also at Tomsk State University, Tomsk, Russia.
- ^k Also at Università di Napoli Parthenope, Napoli, Italy.
- ^l Also at Institute of Particle Physics (IPP), Canada.
- ^m Also at National Institute of Physics and Nuclear Engineering, Bucharest, Romania.
- ⁿ Also at Department of Physics, St. Petersburg State Polytechnical University, St. Petersburg, Russia.
- ^o Also at Department of Physics, The University of Michigan, Ann Arbor MI, United States.
- ^p Also at Centre for High Performance Computing, CSIR Campus, Rosebank, Cape Town, South Africa.
- ^q Also at Louisiana Tech University, Ruston LA, United States.
- ^r Also at Institutio Catalana de Recerca i Estudis Avancats, ICREA, Barcelona, Spain.
- ^s Also at Graduate School of Science, Osaka University, Osaka, Japan.
- ^t Also at Department of Physics, National Tsing Hua University, Taiwan.
- ^u Also at Institute for Mathematics, Astrophysics and Particle Physics, Radboud University Nijmegen/Nikhef, Nijmegen, Netherlands.
- ^v Also at Department of Physics, The University of Texas at Austin, Austin TX, United States.
- ^w Also at Institute of Theoretical Physics, Ilia State University, Tbilisi, Georgia.
- ^x Also at CERN, Geneva, Switzerland.
- ^y Also at Georgian Technical University (GTU), Tbilisi, Georgia.
- ^z Also at O Chadai Academic Production, Ochanomizu University, Tokyo, Japan.
- ^{aa} Also at Manhattan College, New York NY, United States.
- ^{ab} Also at Hellenic Open University, Patras, Greece.
- ^{ac} Also at Academia Sinica Grid Computing, Institute of Physics, Academia Sinica, Taipei, Taiwan.
- ^{ad} Also at School of Physics, Shandong University, Shandong, China.
- ^{ae} Also at Moscow Institute of Physics and Technology State University, Dolgoprudny, Russia.
- ^{af} Also at Section de Physique, Université de Genève, Geneva, Switzerland.
- ^{ag} Also at Eotvos Lorand University, Budapest, Hungary.
- ^{ah} Also at International School for Advanced Studies (SISSA), Trieste, Italy.
- ^{ai} Also at Department of Physics and Astronomy, University of South Carolina, Columbia SC, United States.
- ^{aj} Also at School of Physics and Engineering, Sun Yat-sen University, Guangzhou, China.
- ^{ak} Also at Institute for Nuclear Research and Nuclear Energy (INRNE) of the Bulgarian Academy of Sciences, Sofia, Bulgaria.
- ^{al} Also at Faculty of Physics, M.V. Lomonosov Moscow State University, Moscow, Russia.
- ^{am} Also at Institute of Physics, Academia Sinica, Taipei, Taiwan.
- ^{an} Also at National Research Nuclear University MEPhI, Moscow, Russia.
- ^{ao} Also at Department of Physics, Stanford University, Stanford CA, United States.
- ^{ap} Also at Institute for Particle and Nuclear Physics, Wigner Research Centre for Physics, Budapest, Hungary.
- ^{aq} Also at Flensburg University of Applied Sciences, Flensburg, Germany.
- ^{ar} Also at University of Malaya, Department of Physics, Kuala Lumpur, Malaysia.
- ^{as} Also at CPPM, Aix-Marseille Université and CNRS/IN2P3, Marseille, France.
- ^{at} Also affiliated with PKU-CHEP.
- ^{*} Deceased.